JOURNAL OF GEOPHYSICAL RESEARCH, VOL. 103, NO. D11, PAGES 13,615-13,634, JUNE 20, 1998

Intercomparison of NO, NO_2, NO_y, O_3, and RO_x measurements during the Oxidizing Capacity of the Tropospheric Atmosphere (OCTA) campaign 1993 at Izaña

T. Zenker[1,2], H. Fischer[3], C. Nikitas[3], U. Parchatka[3], G. W. Harris[3,4], D. Mihelcic[5], P. Müsgen[5], H. W. Pätz[5], M. Schultz[5,6], A. Volz-Thomas[5], R. Schmitt[7], T. Behmann[8], M. Weißenmayer[8], and J. P. Burrows[8]

Abstract. An informal comparison of NO, NO_2, NO_y, O_3, and RO_x measurements obtained by different instruments and techniques at Izaña in 1993 during the European Oxidizing Capacity of the Tropospheric Atmosphere (OCTA) campaign was performed. For O_3, two UV instruments agree within 7% (95% cl.) limited by a difference in response of 7.0%±0.2% (95% cl.) which likely was caused by O_3 losses in one of the inlet lines. The NO mixing ratios obtained by two NO/O_3 Chemiluminescence (CL) instruments range between 0-200 parts per trillion by volume (pptv), except for short periods influenced by traffic pollution. The response of the two CL detectors agrees within 3%±10% (95% cl.). The NO_y data, ranging between 100 pptv and several ppbv in plumes, were obtained using two different gold-CO-converters and inlet designs with subsequent CL detection of NO. A systematic difference in the slope between the two data series of 1.44±0.05 (95% cl.) was likely caused by NO_y losses in the inlet line of one of the instruments. Three different NO_2 data sets were obtained using Tunable Diode Laser Absorption Spectroscopy (TDLAS), a photolytic converter/CL technique (PLC/CL), and the Matrix Isolation Electron Spin Resonance (MIESR) technique. The linear slopes between the data sets of the three methods are consistent with unity at a 95% confidence level, 1.13±0.30 (TDL versus PLC/CL), 0.90±0.47 (TDL versus MIESR), and 1.04±0.34 (PLC/CL versus MIESR). RO_x measurements were performed by three different chemical amplifier (CA) designs and the MIESR technique. Using 30-min averaged values between 13-65 pptv, two CA instruments agree within 25% (95% cl.) with the mean of MIESR (1.01±0.20 and 0.98±0.24, 95% cl.), while the third CA responded low (0.65±0.32, 95% cl.).

1. Introduction

In August 1993 a ground based study at Izaña (Tenerife) was performed as part of the Oxidizing Capacity of the Tropospheric Atmosphere (OCTA) project [*McKenna et al.*, 1995]. The objective of this campaign was to study photochemical processes which control the ozone budget and other key photochemical components which influence the oxidation of trace gases in the remote, unpolluted free troposphere. NO, NO_2, NO_y, PAN, CO, HCHO, NMHC, O_3, H_2O_2, and RO_x measurements were carried out at the site (2370 m asl.) in order to obtain a comprehensive data set supplying additional insight into the composition of the remote troposphere which should be suitable for performing further modeling studies on tropospheric photochemistry. Only a few campaigns have obtained comprehensive data sets in the remote troposphere, for example, the Mauna Loa Observatory Photochemistry Experiments (MLOPEX 1 and 2) [*Ridley and Robinson*, 1992; *Atlas and Ridley*, 1996] and NASA's Pacific Exploratory Mission-West A (PEM-West A) [*Hoell et al.*, 1996]. An overview of the measurements and a description of the campaign are presented in *Fischer et al.* [this issue], and the meteorological conditions during the measurement period are described by E. Cuevas (unpublished manuscript, 1997). A detailed analysis of the local photochemistry at the site is discussed by A. Volz-Thomas et al. (Photochemical budgets of peroxy radicals (HO_2 and RO_2) and ozone during the OCTA intensive, submitted to Journal of Geophysical Research, 1997, hereinafter referred to as Volz-Thomas et al., submitted manuscript, 1997), and photochemical aspects of long-range transport are investigated by *Schultz et al.* [this issue].

The intention of this campaign was not to perform a formal blind intercomparison of measurements and techniques, nevertheless, measurements of NO, NO_2, NO_y, O_3, and RO_x were obtained by two or more groups, so that an informal intercom-

[1]Air Chemistry Department, Max-Planck-Institut für Chemie, Mainz, Germany, and Department of Physics, Hampton University, Hampton, Virginia.
[2]Now at Department of Physics, Hampton University, and NASA Langley Research Center, Hampton, Virginia.
[3]Air Chemistry Department, Max-Planck-Institut für Chemie, Mainz, Germany.
[4]Now at Centre for Atmospheric Chemistry, York University, North York, Ontario, Canada.
[5]Institut für Chemie der belasteden Atmosphäre, Forschungszentrum Jülich, Jülich, Germany.
[6]Now at Center for Earth & Planetary Sciences, Harvard University, Cambridge, Massachusetts.
[7]Meteorologie Consult GmbH, Glashütten, Germany.
[8]Institut für Umweltphysik, Universität Bremen, Bremen, Germany.

Paper number 97JD03739.
0148-0227/98/97JD-03739$09.00

parison study is possible. Earlier NO and NO_x intercomparisons have been reported from a ground-based campaign near Boulder, Colorado, [*Fehsenfeld et al.*, 1987] and the NASA Chemical Instrumentation Test and Evaluation (CITE) missions [*Hoell et al.*, 1985, 1987, 1990]. Intercomparisons of NO_y field measurements have been performed during the Boulder campaign [*Fehsenfeld et al.*, 1987] and between ground-based data from MLOPEX 2 and airborne data from PEM-West A [*Atlas et al.*,1996]. Finally, the RO_x intercomparison reported here, is the first performed during a field measurement campaign.

2. Instrumentation

2.1. Measurement Techniques

Three independent NO/O_3 Chemiluminescence Detectors [*Drummond et al.*, 1985] (modified ECOPHYSICS CLD 770 AL ppt) were operated for the in situ measurement of NO/NO_x/ NO_y by Forschungszentrum Jülich, Institut für Chemie der belasteten Atmosphäre and Metereologie Consult GmbH (KFA and MC) (Volz-Thomas et al., submitted manuscript, 1997), one for direct NO detection, one fitted with a broadband photolytical converter (Tecan PLC 760 photolytical converter) to convert NO_2 to NO and measuring NO_x (NO_2 + NO) [*Kley and McFarland*, 1980]. The third CLD was fitted with a NO_y to NO catalytic converter (Au surface at 573 K, 0.3% CO as reducing agent) [*Bollinger et al.*, 1983, *Fahey et al.*, 1985] to detect the total reactive nitrogen species, NO_y. Additionally, NO_2 was determined by the KFA Matrix Isolation Electron Spin Resonance (MIESR) technique [*Mihelcic et al.*, 1985, 1990], with a total of 23 cryogenic samples being taken and analyzed in the laboratory. NO and NO_y measurements by the Max-Planck-Insitut für Chemie (MPIC) were performed using a single NO/O_3 Chemiluminescence Detector (Tecan CLD 770 ppt) and a NO_y to NO converter (Au surface at 573 K, 1% CO as reducing agent) [*Bollinger et al.*, 1983; *Fahey et al.*, 1985]. MPIC NO_2 measurements were obtained using one channel of a four channel Tunable Diode Laser Absorption Spectrometer (TDLAS) [*Roths et al.*, 1996]. For O_3 measurements two UV-absorption instruments were operated, one by MPIC and the other by KFA jointly with MC and the Institute National Metereological (INM) (Thermo Environment Model 49 and Dasibi 1008, respectively). RO_x measurements were performed using three chemical amplifiers (CA) [*Cantrell and Stedman*, 1982; *Hastie et al.*, 1991] and the MIESR technique. The CAs were operated by three different groups from the MPIC, the KFA-ICG2, and the Institut für Fernerkundung, University Bremen (IFE). The chemical amplification of the RO_x signal is based on a catalytic chain reaction. After two initial reaction steps, $RO_2 + NO \rightarrow RO + NO_2$ and $RO + O_2 \rightarrow R'CHO + HO_2$ which are required for organic peroxy radicals only, the HO_2 radical quantitatively converts NO into NO_2 in the catalytic chain reaction $HO_2 + NO \rightarrow OH + NO_2$ and $OH + CO + O_2 \rightarrow HO_2 + CO_2$. The ratio between generated NO_2 molecules and initial HO_2 radicals is defined as the chain length of the CA and is typically of the order of 100. The NO_2 mixing ratios in the ppbv range are then detected by Luminox detectors (MPIC and KFA: Type LMA3, Unisearch; the IFE detector is homemade and similar to the commercial LMA3). The detectors are insensitive toward the NO which is added in ppmv amounts to drive the chain reaction. With the MIESR technique, HO_2 and the sum of higher organic peroxy radicals can be analyzed separately in the ESR spectrum. The setup of the instrumentation at the site and an experimental overview is described in more detail by *Fischer et al.* [this issue]. The measurement techniques relevant for this intercomparison study are summarized in Table 1.

2.2. Sampling and Inlet Designs

An important difference between the KFA and MPIC instrument setups (except the RO_x devices) was the different height of the air sampling points above ground. The air intakes for the KFA in situ instruments as well as the cryogenic sampler for the RO_x/NO_2 MIESR samples and all RO_x CA systems were positioned on top of the building, 2.5 m above the flat roof which is used as an instrumentation platform, at a total height above ground of about 15 m. The air intake point for the MPIC instruments was 2 m above the MPIC measurement trailer, about 5 m above ground and separated by 20 m from the building.

The common Izaña inlet manifold which is permanently in use by INM and MC consists of a stainless steel pipe (60 mm ID, 3 m long) followed by a glass tube (60 mm ID, 30 cm long) to which the different KFA/MC NO, NO_x, and NO_y instruments were connected through PFA tubes (4 mm ID, about 4 m long). A constant flow was pumped through the Izaña inlet line and the manifold so that the residence time of the air was 2 s, and additionally, 1-2 s in the connecting PFA tubes to the individual instruments. A NO_y to NO converter was mounted in front of the MC CL detector. The converter is made of a gold pipe (4 mm ID, 35 cm long) which is inserted into a glass pipe (8 mm ID, 50 cm long). The entire converter is heated to an operating temperature of 573 K. This design has already been used at Schauinsland [*Volz-Thomas et al.*, 1997] and during field campaigns [*Harder et al.*, 1995]. PFA inline filters (Ø = 47 mm, pore size 0.45 μm) were inserted after the glass manifold, before the photolytic converter (KFA) and behind the NO_y converter (MC) and ahead of the third CL detector (KFA) to prevent aerosol contamination of the devices. At a fourth manifold port the INM/MC UV-Ozone instrument was connect through a PFA tube.

The single MPIC CL detector was connected to two different inlet lines, suited either for NO_y or NO measurements. A set of magnetically driven PFA valves selected one of the lines as the active inlet while the other line was bypass pumped, maintaining the same mass flow as the active line. The bypass flow was controlled by a feedback loop consisting of a mass flow meter behind the CL detector, a mass flow controller in front of the bypass pump, and an electronic feedback-integration (FI) circuit. A PFA tube ($^1/_8$ inch ID, 8 m long) was used as NO inlet line with a PFA inline filter connected in front (Ø = 47 mm, pore size 0.5 μm) to prevent a dust and aerosol contamination of the inlet line and instrument. The MPIC NO_y inlet consisted of a NO_y to NO converter followed by a PFA inline filter and a PFA tube similar to the NO inlet. The MPIC NO_y converter is a compact stand-alone assembly which has been operated during airborne [*Zenker et al.*, 1996, *Fischer et al.*, 1997], ground-based [*Zitzelsberger*, 1997; B. Bonsang, manuscript in preparation, 1997], and laboratory studies [*Johnson et al.*, 1996]. The 70 cm long gold pipe (5 mm ID, 6 mm OD), mounted inside a stainless steel housing and vacuum shielding, is heated over a 20 cm long section near its center to 573 K controlled by a temperature sensor feedback

Table 1. Intercomparison Instruments and Periods

Species	Instruments	Data Period of Intercomparison	Duty Cycle[a], %	Time Resolution, min
O_3	Dasibi 1008 (MC)	Aug. 12-22	50	10
	Thermo Environment, M-59 (MPIC)		50	1
NO	Eco Physics CLD[b] 770 AL ppt (KFA)	Aug. 12-22	47	1
	Tecan CLD 779 AL ppt (MPIC)		23[c]	1[c]
NO_y	Eco Physics CLD[b] 770 AL ppt and NO_y to NO converter (KFA)	Aug. 16-20	47	(10), 1[d]
	Tecan CLD 770 AL ppt and NO_y to NO converter (MPIC)		23	1
NO_2	Tecan PLC[e] 760 and Eco Physics CLD[b] 770 AL ppt (KFA)	TDLAS versus PLC/CLD: Aug. 19-20	47	(10), 1[d]
	TDLAS[f], NO_2 channel (1 of 4)	versus MIESR (23 samples):	20[h]	2
	MIESR[g] (KFA)	Aug. 14-21	100	30
RO_x	RO_x-CA[i], (IFE)	Aug. 14-21	50	1
	RO_x-CA (MPIC)		50	1
	RO_x-CA (KFA)		50	1
	MIESR[g] (KFA)		100	30

Listed are the different instrument sets per species for which the measurement intercomparisons have been performed, along with intercomparison periods and instrument parameters.

[a]Duty cycles are approximately values which depend of the actual timing of the instrument operation which in some cases has changed during the investigated time period.

[b]Chemiluminescence Detector.

[c]Under standard operation the CLD itself has a duty cycle of 46.7% (1-min integration and 1 s purge times), but since the MPIC NO and NO_y inlet lines are toggled, the duty cycle reduces to 23.4% on average. The inlet lines were switched every 5 min.

[d]10 min before August 16, afterward 1 min.

[e]Photolytical Converter.

[f]Tunable Diode Laser Absorption Spectrometer.

[g]Matrix Isolation Electron Spin Resonance.

[h]Duty cycle is variable, for example, 20% represents a series of 3 ambient measurements and one zero gas measurement each over 2 min with purge time between the ambient and zero gas measurements of 1 min each. This results in a 80% duty cycle, but accounting for time sharing equally between four channels of one measured species each, this reduces to 20%. Although, the duty cycle is effectively slightly larger since the smallest measurement interval of 3 s between switching channels is effectively longer due to an 3/e-exchange time of the White cell of typically 1 s (see [*Fischer et al.*, 1996 this issue, and *Roths et al.*, 1996].

[i]Chemical Amplifier

loop. The air is directly sampled into the gold pipe. The temperature at the front end of the gold pipe is typically 373 K for mass flows of 1.5 standard liter per minute (slm). About 5 cm after the inlet point, stainless steel tubes are connected to the straight gold pipe to supply the reducing agent CO, and when needed, zero and calibration gases. For the UV O_3 instrument and the TDL spectrometer PFA tubes were used ($^1/_8$ inch ID and $^3/_8$ inch ID, respectively) with PFA inline filters (∅ = 47 mm, pore size 0.5 μm) mounted at the front of the inlets. Zero and calibration gases for the TDL instrument could be added through PFA manifolds in front of the filter [*Fischer et al.*, this issue]. All PFA inlet lines and PFA calibration gas supply lines were wrapped in black tubing and guided inside a stainless steel pipe into the trailer.

The RO_x (CA) instruments from the MPIC and IFE are similar in design to that described by *Hastie et al.* [1991], while the KFA CA has a new inlet design [*Schultz*, 1995]. The main difference between these two types is the design of the inlet section where the reaction agents are added and the chain reaction starts. The IFE and MPIC inlets consist of a short, ~3 cm, PFA tube ($^1/_4$ inch OD) in front of a PFA T-connector followed by a PFA tube ($^1/_4$ inch OD; IFE and MPIC used thick and thin walled tubes, respectively). Through the T-connector, the NO and CO agents are added. The KFA design is a double wall stainless steel pipe. At the front end the NO gas is added to the airflow through a 360° circular slit so that the inside wall is shielded with a flow of high concentration NO, minimizing initial radical wall loss reactions.

Calibrations and intercomparisons of calibration standards are described in the subsequent section as part of the intercomparison study. For simplification, all equipment and instruments with responsibilities by KFA, MC, or INM (see this section and Table 1) will be indicated with KFA in the following text since KFA carried out the measurements.

3. Data Intercomparison and Discussion

3.1. General Remarks

3.1.1. Data sets. The data discussed here, are compared at their original time resolution of 1 min in the case of NO, NO_y and O_3 as well as in their 30-min averages as published on a CD-ROM database [*Stordal et al.*, 1995]. Table 1 summa-

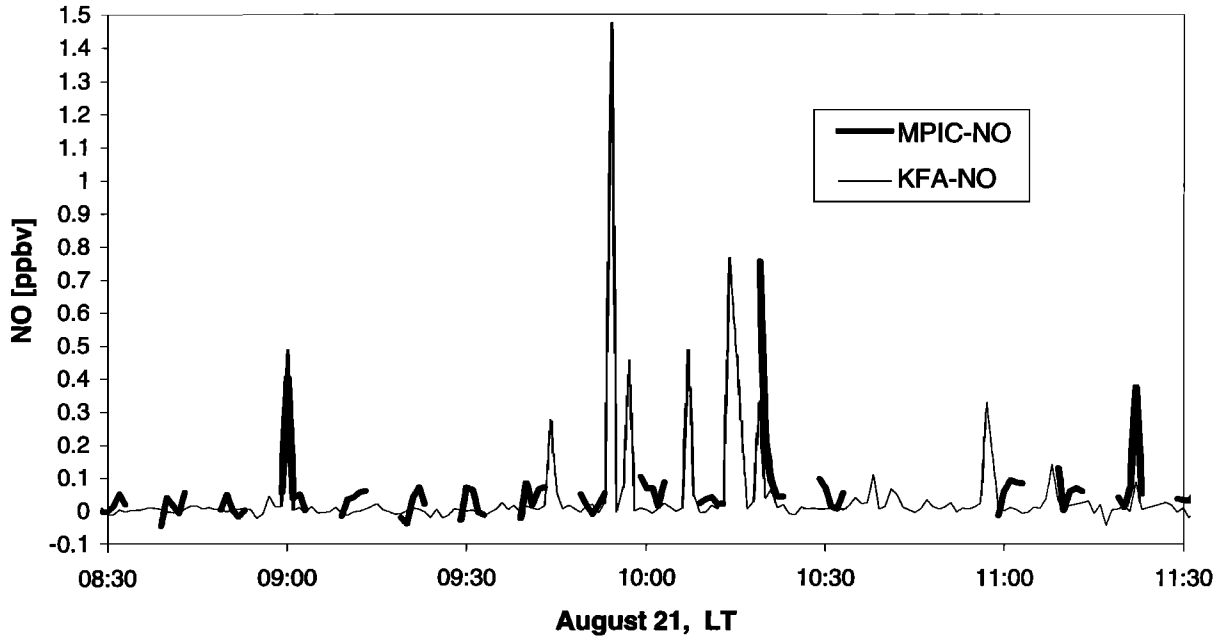

Figure 1. Time series of NO measurements performed by the KFA and MPIC instruments (see Table 1) between 0830 and 1130 LT on August 21. Several traffic pollution spikes are apparent. Five min MPIC data gaps result from the single CL detector measurements switching between the NO and NO_y inlet lines; the gap between 1030 and 1100 LT results from a NO calibration sequence.

rizes the species, instruments, time periods, duty cycles, and time resolutions.

Occasionally, short spikes of enhanced NO, NO_2, and NO_y mixing ratios appear in the data series which originate from traffic exhaust plumes, mostly generated by single cars (less than 60 per hour) along a road which passes about 500 m north of the site, and upwind under upslope conditions [*Fischer et al.*, this issue]. Many spikes consist only of one data point and many are seen only by one of the NO, NO_2 or NO_y instruments which were operated at an 1-min time resolution (2-min for TDLAS) and which had duty cycles below 50%. An example of recorded and missed pollution spikes is illustrated in Figure 1 displaying a NO time series measured by the MPIC and KFA instruments. Both instruments recorded a NO spike at 0900 LT, while nearly all spikes between 0940 and 1100 LT seen by the KFA instrument have been missed by the MPIC instrument. These spikes fall into 5 min data gaps which are apparent in the MPIC NO data. The MPIC NO and NO_y measurements were performed using one CL detector switching between the two inlet lines every 5 min. The very last spike in this data series, at 1120 LT, was recorded by both instruments but appears much smaller to the KFA instrument, which can be explained by the <50% duty cycle of the CL detectors. The majority of the pollution spikes occurred between sunrise and noon each morning. Spikes seen only by one of the instruments were always excluded from the intercomparison of the data series at their original time resolution. In the 30-min averaged database the pollution spikes had generally been included since these data should reflect the observed averaged mixing ratios at the measurement site.

3.1.2. Statistical tools. Pairs of data series are compared by their mean values and their linear relationship which is analyzed using linear fit routines as described by *Press et al.* [1996]. Two data series, x and y, are fitted using a χ^2 fit to a straight line $y = i + sx$ (routine fitexy of *Press et al.* [1996]) with errors in both variables, x and y. For a best fit result the routine's goodness-of-fit parameter χ^2 and the probability Q for a value of χ^2 occurring equal or higher than the computed one will be $\chi^2 = df = n-2$ and $Q = 0.5$, respectively, where df are the degrees of freedom and n are the number of data pairs. Low values of χ^2 and high values of Q are likely due to overestimated errors in x and y, while the opposite can be the results of an inappropriate straight line model or an underestimation of the errors in x and y; furthermore, a tail of outliers will lower the χ^2 value. The standard deviations σ_s and σ_i for slope s and intercept i, respectively, depend not only on the degree of linear correlation between the data but also depend on the size of the errors in x and y. In particular, scaling the x and y error linear up and down will increase and decrease the slope and intercept error, respectively, without changing the most likelihood result of the two fit parameters, s and i. A measure of an acceptable size of the errors in x and y are the χ^2 and Q values, as discussed by *Press et al.* [1996]. These will determine whether the fit result and its errors are acceptable. Q should yield values close to 0.5, where $Q = 10^{-3}$ might be still acceptable, but, especially the errors of the fit parameters, are not acceptable when Q reaches 10^{-18} or unity. For each of our fits we will first report the resulting error limits for slope and intercept based on our estimated data variability and, second, based on scaling the errors linear to approach the best fit scenario. The latter errors (standard deviation σ) for the best fit scenario can be calculated by multiplying the resulting σ values with the factor $\chi/\sqrt{n-2}$ [*Press et al.*, 1996]. As a worst case scenario, we report as a final error the larger of the two at a 95% confidence level; this is $x \pm 1.96 \times \sigma_x$.

The correlation of the two data samples is evaluated by the regression coefficient r_S which is calculated using Spearman's

Table 2. Summary of Statistics on the Measurement Intercomparisons

Species		Data Samples			χ^2 Linear Fit - Linear Correlation						
Data Range Period	Time, min	Method(Group): Ratio(Group/Group):	Mean Ratio of Mean	95% cl.	$y(x)$ Number of Points χ^2 (Q)	Slope	95% cl. (Best Fit)	Intercept	95% cl. (Best Fit)	r_S (r_S^2)	Nonzero Probabiliy, %
O_3, ppbv		UV(MPI):	49.0	± 0.2	KFA(MPI)						
24-77 ppbv	1	UV(KFA):	46.6	± 0.2	14,400	0.933[c]	± 0.002	0.91[b]	± 0.22	0.992	>99.9[a]
Aug. 12-21		ratio(KFA/MPI):	0.96[c]	± 0.01	3,458 (1.0)[b]		(± 0.001)		(± 0.11)	(0.984)	
O_3, ppbv		UV(MPI):	52.3	+1.0/-1.2	KFA(MPI)						
26-72 ppbv	30	UV(KFA):	49.6	+0.9/-1.1	384	0.945[c]	± 0.014	0.24[a]	± 0.77	0.995	>99.9[a]
Aug. 12-21		ratio(KFA/MPI):	0.95[c]	± 0.04	81 (1.0)[b]		(± 0.007)		(± 0.35)	(0.991)	
NO, pptv		CLD(MPI):	42.9	+2.1/-1.7	MPI(KFA)						
<200 pptv	1	CLD(KFA):	28.0	+1.7/-1.0	4,073	0.97[a]	± 0.10	16[b]	± 5	0.58	>99.9[a]
		ratio(MPI/KFA):	1.53[b]	± 0.09	614 (1.0)[b]		(± 0.03)		(± 1)	(0.34)	
NO, pptv		CLD(MPI):	53.2	+2.6/-1.5	MPI(KFA)						
0-5.8 ppbv	1	CLD(KFA):	38.0	+2.3/-1.1	4,159	1.09[b]	± 0.03	12[b]	± 4	0.61	>99.9[a]
		ratio(MPI/KFA):	1.40[b]	± 0.05	403 (1.0)[b]		(± 0.01)		(± 1)	(0.37)	
NO_y, ppbv		Au-CLD(MPI):	0.730	± 0.020	MPI(KFA)						
0.1-4.0 ppbv	1	Au-CLD(KFA):	0.589	± 0.015	1,686	1.44[c]	± 0.05	-0.082[b]	± 0.022	0.93	>99.9[a]
Aug. 16-20		ratio(MPI/KFA):	1.24[c]	± 0.04	462 (1.0)[b]		(± 0.03)		(± 0.011)	(0.86)	
NO_y, ppbv		Au-CLD(MPI):	0.84	+0.11/-0.06	KFA(MPI)						
0.1-2.9 ppbv	30	Au-CLD(KFA):	0.82	+0.11/-0.06	164	0.95[a]	± 0.06	0.000[a]	± 0.062	0.93	>99.9[a]
Aug. 16-20		ratio(MPI/KFA):	1.02[a]	± 0.19	91 (1.0)[b]		(± 0.05)		(± 0.047)	(0.86)	
NO_2, pptv[d]		PLC/CLD(KFA):	253	± 71	PLC(ESR)						
55-672 pptv	30	TDL(MPI):	331	± 75	16	1.04[a]	± 0.10	-70[b]	± 33	0.82	>99.9[a]
Aug. 14-21		MIESR(KFA):	314	± 59	154 ($<10^{-18}$)[b]		(± 0.34)		(± 110)	(0.67)	
		ratio(PLC/ESR):	0.81[a]	± 0.27	TDL(ESR)						
		ratio(TDL/ESR):	1.05[a]	± 0.31	18	0.90[a]	± 0.39	-3.6[a]	± 128	0.67	99.7[a]
		ratio(TDL/PLC):	1.31[a]	± 0.47	24 (0.1)[a]		(± 0.47)		(± 155)	(0.44)	
					TDL(PLC)						
					11	0.71[a]	± 0.38	151[a]	± 114	0.69	98.1[a]
					17 (0.05)		(± 0.53)		(± 157)	(0.48)	

Table 2. (continued)

Species		Data Samples			χ^2 Linear Fit - Linear Correlation						
Data Range Period	Time, min	Method(Group): Ratio:	Mean Ratio of Means	95% cl.	$y(x)$ Number of Points χ^2 (Q)	Slope	95% cl. (Best Fit)	Intercept	95% cl. (Best Fit)	r_S (r_S^2)	Nonzero Probabiliy, %
NO_2, pptv		PLC/CLD(KFA):	133	+19/-17	TDL(PLC)						
-16-544 pptv	30	TDL(MPI):	151	+23/-22	74	1.13[a]	± 0.30	2[a]	± 46	0.83	>99.9[a]
Aug. 14-21		ratio(TDL/PLC):	1.14[a]	± 0.29	19 (1.0)[b]		(± 0.16)		(± 23)	(0.69)	
RO_x, pptv		CA/L(IFE):	23.2	+3.8/-3.6	IFE(MPI)						
-15-94 pptv	30	CA/L(MPI):	11.7	+2.5/-2.1	159	1.93[c]	± 0.19	0.5[a]	± 3.0	0.76	>99.9[a]
Aug. 14-21		ratio(IFE/MPI):	1.98[c]	± 0.36	298(0.09)[a]		(± 0.26)		(± 4.2)	(0.57)	
		CA/L(IFE):	24.8	+4.1/-4.0	IFE(KFA)						
		CA/L(KFA):	25.2	+4.9/-4.5	134	0.86[b]	± 0.05	3.1[b]	± 1.8	0.72	>99.9[a]
		ratio(IFE/KFA):	0.98[a]	± 0.35	703($<10^{-18}$)[b]		(± 0.13)		(± 4.2)	(0.52)	
		CA/L(MPI):	16.4	+3.4/-3.1	MPI(KFA)						
		CA/L(KFA):	30.0	+5.1/-5.3	109	0.56[c]	± 0.07	-0.6[a]	± 2.8	0.83	>99.9[a]
		ratio(MPI/KFA):	0.55[c]	± 0.37	94 (0.82)[a]		(± 0.07)		(± 2.6)	(0.70)	
RO_x, pptv[e]		CA/L(IFE):	47.8	+5.0/-3.9	IFE(MIESR)						
13-65 pptv	30	MIESR(KFA):	47.3	+5.4/-5.1	18	0.59[b]	± 0.53	20[a]	± 25	0.66	99.7[a]
Aug. 14-21		ratio(IFE/ESR):	1.01[a]	± 0.20	5.1 (1.0)[b]		(± 0.30)		(± 14)	(0.44)	
		CA/L(MPI):	28.2	+4.9/-4.2	MPI(MIESR)						
		MIESR(KFA):	43.4	+7.8/-5.6	8	0.45[b]	± 1.06	9[a]	± 45	0.73	96.0[a]
		ratio(MPI/ESR):	0.65[b]	± 0.32	0.8 (0.99)[b]		(± 0.40)		(± 17)	(0.53)	
		CA/L(KFA):	42.1	+4.1/-4.4	KFA(MIESR)						
		MIESR(KFA):	43.1	+6.0/-5.8	11	0.55[b]	± 0.38	19[b]	± 17	0.65	97.0[a]
		ratio(KFA/ESR):	0.98[a]	± 0.24	9.3 (0.41)[a]		(± 0.38)		(± 17)	(0.42)	

Ratios of means, parameters resulting from the χ^2 fit (χ^2 (Q), slope, intercept), and the nonzero probability of the correlation coefficient r_S are footnoted to indicated their significance on a 95% confidence level as specified below.

[a]No evidence of, for example, biases or insignificant correlation between data series (95% cl.).

[b]Results indicate a >95% probability of, for example, linear or constant biases (slope and intercept, respectively) or different mean values, or other results which need further discussion in the text. However, deviations can be explained within instrument or calibration specifications. Thus instrument biases are not evident.

[c]In contrast, these results indicate, for example, slopes significantly different from unity which cannot be explained within the instrument specification or calibration accuracy. Thus instrument biases or sampling problems are evident on a 95% confidence level.

[d]The means and ratios of the means given for the NO_2 comparison between the 3 methods PLC/CLD, TDL, and MIESR include only those 11 30-min data averages which are recorded by all 3 methods, while the χ^2 fits include all data pair for each of the compared two methods.

[e]The statistics quoted for the CA versus MIESR comparison does not include high ESR samples (see text).

(nonparametric) rank-order correlation (routine spear of *Press et al.* [1996]). A nonparametric correlation is the most critical test for a correlation of two data series. The probability of nonzero r values are computed according to the spear routine.

In addition to the linear fit analysis, the data are compared by the 95% confidence intervals of their mean values. This is equivalent to a straight line fit forced through the origin. The 95% confidence intervals of the mean $\bar{x} \pm \sigma_m$ are computed as $\sigma_m = t_{0.025,n-1} \times \sigma/\sqrt{n}$, where σ is the standard deviation of the sample x_i, $i = 1,...,n$, and $t_{0.025,n-1}$ is the 2.5% point of the t-distribution. For example, $t_{0\,025,9} = 2.228$, $t_{0\,025,119} = 1.98$, which converges for $n \to \infty$ to the value of the 2.5% point of the standard distribution, equal to 1.96. Some of the data samples obtained during this campaign include data points of elevated mixing ratios which stretch the overall data distribution unsymmetrically towards the higher concentration end, making the overall distribution differ from a normal distribution. In order to achieve a better estimate of the confidence interval of the mean, σ_m is estimate on either side of the mean as the maximum of the computed standard deviation, the range between the mean and the 68 percentage point, and the half range between the mean and the 95 percentage point (for a normal distribution these values will be identical). This results in an upper limit for σ_m, for example, if the apparent maximum is the range mean - 68 percentage point then the estimated σ_m value represents a distribution of the current number of data points within the 68 percentage range and with a 95 percentage range filled up with missing data compared to a normal distribution. Two independent σ_m values are always computed for the half distributions below and above the mean. All results of the statistical analysis which will be discussed below are summarized in Table 2.

3.2. Ozone (O_3)

3.2.1. Data sets. The original MPIC and KFA O_3 data were obtained in a 1-min and 10-min resolution, respectively. A 1-min data set was generated from the KFA data applying a cubic spline interpolation, and 10-min and 30-min data sets were generated by averaging the original data. The estimated errors used as input for the least square fit routine are ±1 ppbv according to the instrumental specification.

3.2.2. Results. The linear least square fits to the three data sets result in nearly identical slope and intercept values for the KFA data against the MPIC data series, for example, the 1-min and 30-min data slopes are 0.933±0.002 and 0.945±0.014, respectively, with intercepts of 0.91±0.22 and 0.24±0.77 ppbv (see). The intercepts lie within the instruments' specifications. On the other hand, the slopes indicate a significant linear bias between the two instruments. This bias correspond to an absolute error of more than 3 ppbv ozone for mixing ratios greater than 43 ppbv. This is outside the calibration errors of ±1 ppbv stated for each of the two instruments . The rather low χ^2 and high χ^2 probabilities Q (see Table 2) imply that the error estimates are too conservative. A trial reduction of the errors to about 50% produces best fit conditions. The difference of the mean values (Figures 2a and 2b, and Table 2) is consistent with the observed linear and constant biases.

3.2.3. Discussion. Linear least square fits for individual days yield slopes of 0.93, 0.91, 0.91, 0.95, 0.89, 0.92, 0.91, 0.97, 0.95, 0.96, and 0.96 from August 12-21, respectively. An air mass change in the night of August 14-15 was associated with high aerosol loads before August 15 [*Fischer et al.*, this issue]. Conceivably, the high aerosol load could have caused O_3 losses through aerosol contamination of the KFA inlet line, which was not protected by an inline filter. However, no clear dependency of the daily slopes on the aerosol load is evident. The slope increases significantly on August 15 after the aerosol event but then drops again for three days and finally recovers for the last four days, all during a low aerosol load in the measured air. Both instruments were also compared with other units at their home institutes but did not show variations greater than 1 ppbv. Also, it is unlikely that a real gradient between the two sampling points at 5 m and 15 m above ground exists, since the difference persists for day and night time measurements and under different wind conditions. Possible losses in the Izaña inlet line could not be confirmed in tests after the campaign using a second Dasibi instrument, which was placed on the measurement platform without any external inlet line. Differences of less than 1 ppbv were measured between the two instruments. Even though no systematic differences could be verified, losses in the KFA inlet line might have played a role. Those losses might have been no longer detectable on the August 22 when the test of the KFA inlet line was performed. During the last 3 days, August 19-21, the computed slopes between the daily data sets increased to values of 0.95 and 0.96, and at ambient mixing ratios of typically 60 ppbv this corresponds to differences of less than 3 ppbv during these 3 days. On August 22, ambient mixing ratios had dropped to values around 30 ppbv, so that the difference expected from the 4% disagreement was less than 1.5 ppbv. This is within the instrument specifications. Thus, on this day, it was not possible to verify the systematic difference which had been observed between the two data sets.

3.3. Nitric Oxide (NO)

3.3.1. Calibration. For calibration of the CLD's secondary standards were used during the campaign which were then calibrated at the KFA-ICG2 institute against primary standard (BOC 55355, 10.0±0.2 ppmv NO) which in turn had been cross-calibrated with other standards in the past [*Volz-Thomas et al.*, 1996]. It was found that the primary standard used here was 4% low compared to a NOAA standard, agreed within 2% with primary standards from KFA-ICG3 and IFU Garmisch-Partenkirchen, and within 0.5% with a new KFA-ICG2 primary standard (BOC 104851). The secondary NO standards used by KFA and MPIC are factory pre-calibrated tanks, AIRCO CC59552/CC16837 (both nominal 1.94 ppmv, KFA calibrated 1.68±0.03 ppmv) and Linde 107712 (nominal 2.0 ppmv, KFA calibrated 1.82±0.02 ppmv), respectively. Both NO data sets were thus ultimately tied to the same primary standard with a remaining relative uncertainty of 2.1% in response (linear bias) between the KFA and MPIC CL detectors. An offset correction was applied to the KFA data set by subtracting the mean nighttime mixing ratio from the entire data set (-4 and -7 pptv for the two CL detectors used, respectively). The MPIC CLD was less sensitive than the modified KFA units. The variance of 1-min data was occasionally as high as ±80 pptv when the mean nighttime mixing ratios were below 20 pptv (mean between 2100 - 0500 LT 12.6±1.8 pptv, 1σ of the data set is ±46 pptv). Thus an offset correction was not applied because of the large uncertainty in the nighttime MPIC NO data.

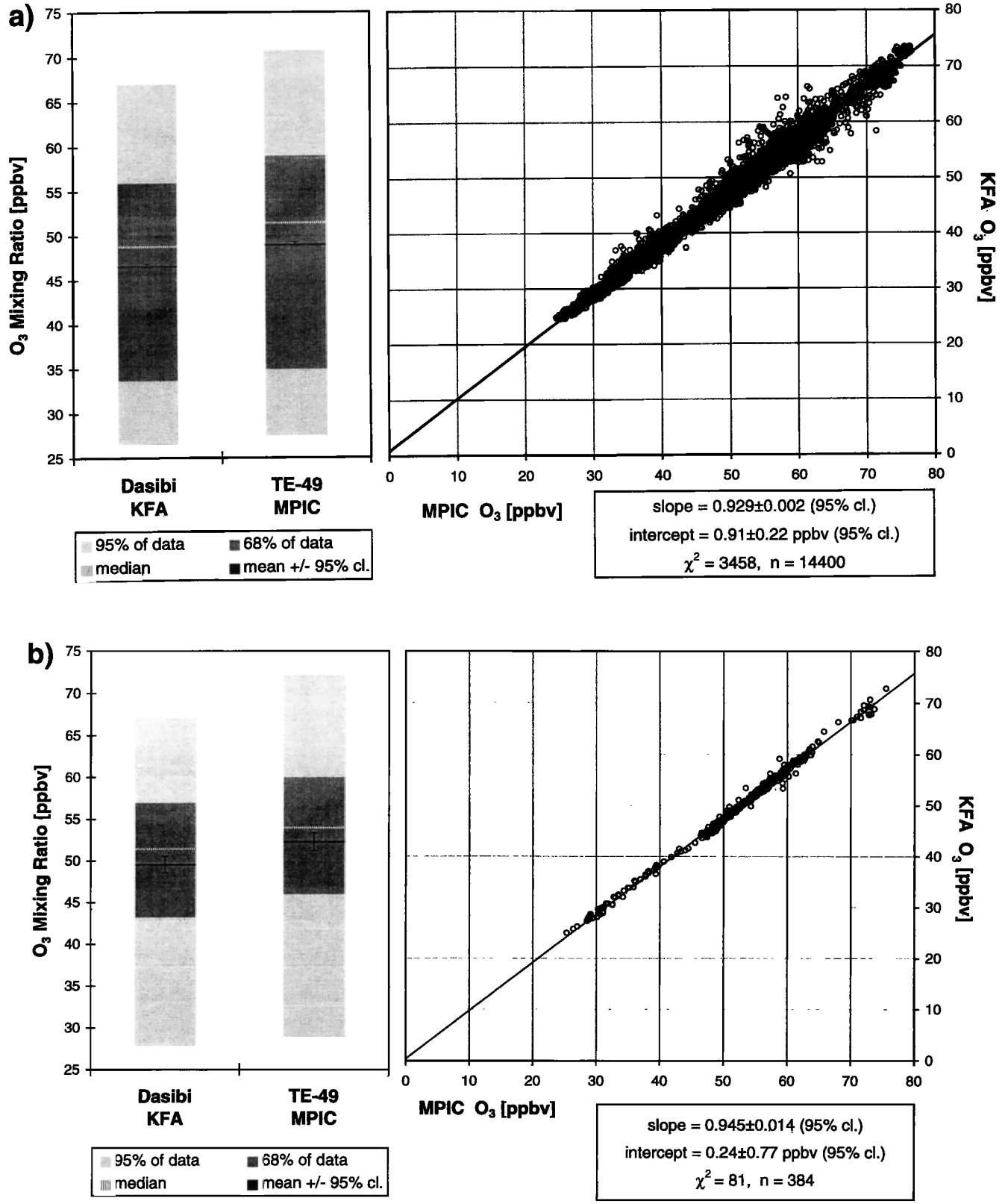

Figure 2. Intercomparison of ozone (O_3) measurements. Data series obtained by the KFA instrument versus the series obtained by the MPIC instrument (see Table 1). Shown are (a) 1-min and (b) 30-min ozone data. (right panel) Scatterplot of the data pairs with fitted line (solid line) through all data points. (left panel) Box and whisker bars of the data samples indicating the mixing ratio intervals for 68% and 95% of the data points, and median and mean values. The 95% confidence intervals of the mean values are displayed by the error bars (see also statistical tools section).

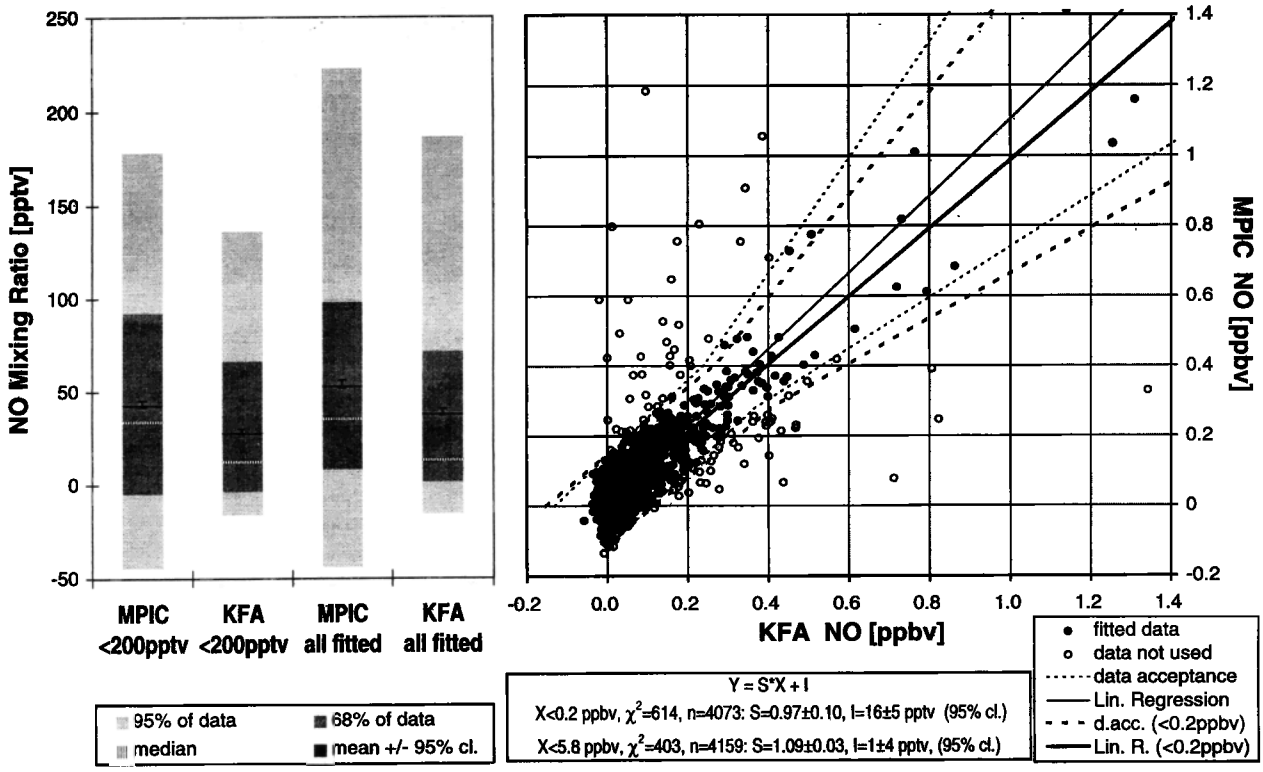

Figure 3. Intercomparison of nitric oxide (NO) measurements. Data series of the 1-min NO data obtained by the MPIC instrument versus the series obtained by the KFA instrument (see Table 1). (right panel) Scatterplot of the data pairs fitted lines (solid line) and data acceptance limits (dashed lines, see also text) separating between data used in the least squares fits (solid circles) and those rejected (open circles). Two linear least squares fits, one over the entire mixing ratio range and the other for data lower than 200 pptv, were computed. Left panel is as in Figure 2.

Both data sets were corrected for NO losses due to the reaction of $NO+O_3 \rightarrow NO_2+O_2$ ($k=2.0\times10^{-12}\times\exp(^{-1400}/_{T[K]})cm^3$ $molecules^{-1}s^{-1}$ [*DeMore et al.*, 1994]) in the inlet line. An exponential decay correction of approximately 2.5% and 4% per 30 ppbv ambient O_3 was applied for the MPIC and KFA data using the known inlet line volume, mass flow, ambient O_3 mixing ratios, a mean temperature and pressure of 297 K and 760 hPa, respectively.

3.3.2. Analysis. All 1-min KFA-MPIC NO data are displayed in Figure 3. Data points with enhanced mixing ratios observed by only one of the instruments are associated with short pollution spikes which were not always detected by both instruments because of their duty cycles.

Pollution spikes seen by both instruments are included in the analysis in order to extend the dynamic range of the data. On the other hand, pollution spikes completely seen by only one of the instruments need to be classified as outliers and were rejected from further analysis. In order to accomplish this the following two alternative acceptance criteria were defined. First, we estimate the overall variance of the measurement by evaluating the total scatter of the data observed at night assuming constant mixing ratios for NO. Applying this information to the entire data set, all data are accepted that deviated from the regression line by less than the total variability observed at night (this is ±10 ppt for KFA and ±100 ppt for MPIC). Second, the data were accepted if they fell into an acceptance angle defined by two straight lines having $^3/_2$ and $^2/_3$ times the slope of the linear fit function. The last criterion ensures that some possible non linearity in one of the instruments would be included without the analysis being disturbed by extreme outliers. The choice of the acceptance angle is somewhat arbitrary, however, the results change only slightly with its variation. Since the acceptance limits are not related to the unity line but are dependent on the actual resulting least squares fit parameters, the data selection and fits were computed iteratively until the final sample of data points met the acceptance criteria. In the case of NO, two different data ranges were considered, the entire range of 1-min mixing ratios (0-5.8 ppbv) and the range between 0-200 pptv where more than 97% of the NO measurements lay. The estimated errors for the χ^2 fit are 10 ppt and 100 ppt for KFA and MPIC data, respectively, based on the observed nighttime variance. These are applied for the 30-min data set, too, instead of using the standard deviations resulting from the averaging. Because of the larger variance of the averages affected by pollution plumes the fit routine would assign a much lower weight to these points but it was the intention to include these data at the high concentration end fully in the extended data set. That data average contains a pollution spikes does not make it less reliable but it does increase the standard deviation of its mean, thus it is misleading to use this averaging variance to weight the data points for this application. Otherwise, these data

points would be under weighted like outliers. The selection of outliers is already handled through the applied acceptance criteria. The acceptance limits and the resulting linear fit lines for the two ranges are indicated in the Figure 3.

3.3.3. Results and discussion. The regression coefficients r_s of only 0.58 (rank-order correlation) for data <200 pptv and its high nonzero probability (see Table 2) reflects the broad MPIC NO scatter band which is almost as wide as the range of mixing ratios considered. The low χ^2 value and the Q probability equal to unity (Table 2) suggest that the error estimates for the data variability are to high. Best fit conditions can be met with an decrease of the errors to 40%. The resulting slope of 0.97±0.10 (±0.03 for best fit conditions) of the linear least square fit for NO mixing ratios lower than 200 pptv is consistent with unity within the 95% confidence limits.

For the comparison over the entire range of mixing ratios, the MPIC data come out significantly higher, with a slope equal to 1.09±0.03. The deviation from unity is caused by the data points at higher mixing ratios since the trend is not apparent below 200 pptv NO. Despite the statistical significance of the result, the number of data points at the high concentrations (>200 pptv) is too low to decide on a possible nonlinearity in this range (compare Figure 3). Thus, the statistical significance of the higher slope for the entire data set compared to data <200 pptv should not be overinterpreted. Moreover, the distance and different heights of the two in situ sampling points may result in a real difference for the traffic spikes, since the road is only 500 m away and plumes might not be well mixed up to a height of 15 m above ground over this short distance.

The significant intercepts of 16±5 pptv and 12±4 pptv, respectively, are likely due to the uncorrected offset in the MPIC NO data set of 12±2 pptv (see above). Obviously this offset is also apparent as a statistically significant difference of the means in the same range, 14.9 pptv and 15.2 pptv, respectively. Offsets in this range are not unusual for CL detectors.

3.4. Total Reactive Nitrogen Oxides (NO_y)

3.4.1. Calibration. The CL instruments used for detection of the NO resulting from the catalytic NO_y to NO conversion were calibrated as described in the previous section. In addition, the NO_y data were corrected for the actual conversion efficiency of the catalytic NO_y to NO converters. This efficiency was determined several times during the campaign for the MPIC and KFA converters with NO_2, using the same NO_2 calibration standards and techniques, a dynamically diluted NO_2 permeation source and a $NO + O_3 \rightarrow NO_2 + O_2$ gas phase titration (GPT), which were used for the calibration of the NO_2 measurements by the TDLAS (MPIC) and by the PLC/CLD (KFA), respectively (see next section). The NO_2 calibration gas was added at the very front of the MPIC converter inlet. For calibration of the KFA converter, the NO calibration gas was partially titrated to NO_2 (with O_3 generated by photolysis of O_2), prior to the dilution step (Volz-Thomas et al., submitted manuscript, 1997). The conversion efficiencies were found to be 80%±5% and 68%±12% for the MPIC and KFA converters, respectively. Unfortunately, the NO_2 permeation source was not tied to the NO standards and we rely on the gravimetric calibration (see NO_2 section). HNO_3 conversion efficiencies were not measured at Izaña but earlier laboratory test always showed the same or slightly (~5%) lower conversion efficiencies for HNO_3 compared to NO_2 for the MPIC device. The HNO_3 conversion efficiency for the less efficient KFA device is not known. There were no preparations in place to test this since the low NO_2 conversion efficiency was rather unexpected. The two data sets were recalibrated to their Institute's primary NO standards and conversion efficiency corrections were applied to the data. Thus a total uncertainty of 13% remains between the data sets (this is the squared sum of the NO intercalibration uncertainty, 2%, and the two NO_2 conversion uncertainties, 5% and 12%). An offset correction has not been applied to either NO_y data set. We see no reason to believe that mixing ratios of <200 pptv observed in zero gas are not real, and they usually vary from tank to tank (Messer Griesheim hydrocarbon free synthetic air; and CO from an Al tank was purified by a charcoal and a J_2 trap).

3.4.2. Analysis. Acceptance criteria for the NO_y data to be used for a linear correlation analysis between the two data series were applied in the same way as for the NO data comparison. The accepted scatter bands around the regression line were estimated from nighttime measurements to be ±200 pptv and ±30 pptv for the MPIC and KFA data in order to include the entire data variability at the low concentration end. They are applied for both the 1 and 30-min data sets (see discussion in the NO section).

3.4.3. Results and discussion. The goodness-of-fit parameter for NO_y (Table 2) likely implies underestimated errors. For instance, if the KFA error is increased by a factor of three, best fit conditions are achieved. This might imply that the variability during daytime is higher than the nighttime variability used in the fit. The 1-min MPIC data remain 44%±5% high (95% cl.) compared to the KFA data (see Figure 4a and Table 2) which cannot be explained by the overall uncertainty between the two data sets of 13% (see above). The most likely explanations for the large discrepancy are that sticky molecules like HNO_3 were at least partly lost in the KFA inlet system before reaching the NO_y converter, and second, since the NO_2 to NO conversion efficiency was only 68%, there may has been a much lower HNO_3 conversion efficiency for the KFA converter. In laboratory tests we observed that in case of low NO_2 efficiencies the HNO_3 conversion becomes relatively more inefficient than for NO_2.

Since the dynamic range of the nighttime data is less than 300 pptv it is not possible to establish a fitted slope value which is precise enough to distinguish between night and daytime response differences of the two instruments. The fitted slopes for daytime (upslope) conditions on individual days between MPIC versus KFA data are 1.46, 1.21, 1.35, 1.69, and 1.31 for August 17-21, respectively. NO_x and peroxyacetyl nitrate (PAN) are the only other species which are included in NO_y and have been measured individually (compare Figure 4b of *Fischer et al.* [this issue]). PAN and NO_x contribute less than 10% and approximately 20-30% to the NO_y amount in this period, respectively [*Fischer et al.*, this issue]. Apparently, on August 17 and 20, the days with the highest NO_y ratios between the MPIC and KFA instruments, the daytime PAN measurements are roughly twice as high as those observed on the other days and NO_x accounts for approximately 25% of MPIC NO_y during daytime upslope conditions and outside of pollution spike periods compared to approximately 30% on August 18 and 19. This suggests higher amounts of HNO_3 and/or other organic nitrogen oxides accompanying the higher PAN observations from local

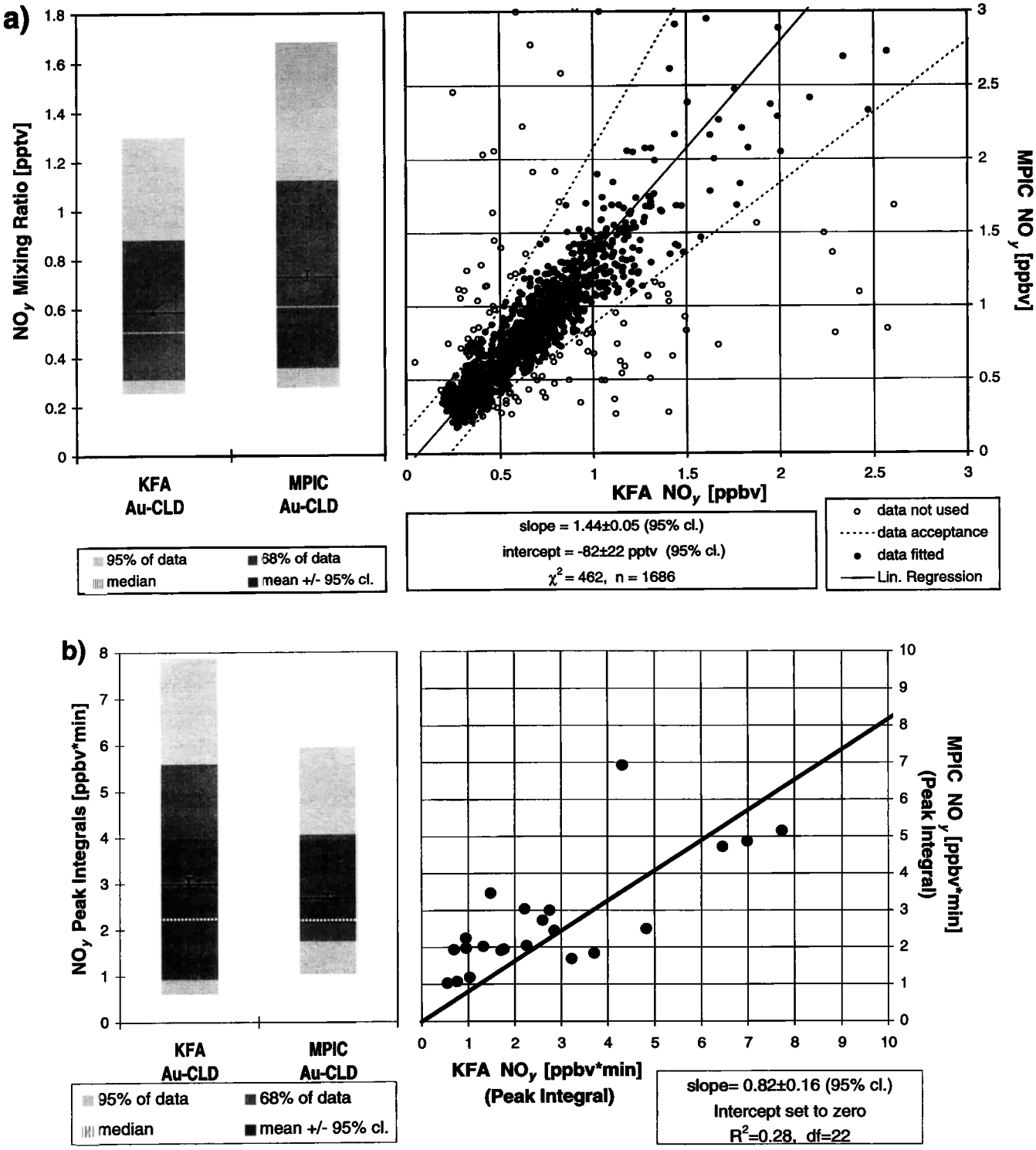

Figure 4. Intercomparison of total reactive nitric oxides (NO_y) measurements. Left and right panels are as in Figure 2. (a) One-min NO_y data series obtained by the MPIC instrument versus the series obtained by the KFA instrument (see Table 1). (b) Integrals of pollution spikes seen by both instruments (KFA and MPIC) versus each other. (c) Shown are 30-min averages of the final NO_y data set along with a linear fit through all data points with a slope close to unity due to an applied correction of the KFA data (see text).

sources on the August 17 and 20, both of which would point toward a detection deficiency of HNO_3 or of higher organic nitrogen oxides of the KFA device compared to the MPIC device. From the available data we can not distinguish what species contributes most. Additionally, the comparison of mean NO_y mixing ratios of pollution spikes seen by both instruments (Figure 4b) showed almost the same response for both of the instruments, with even a tendency for the MPIC

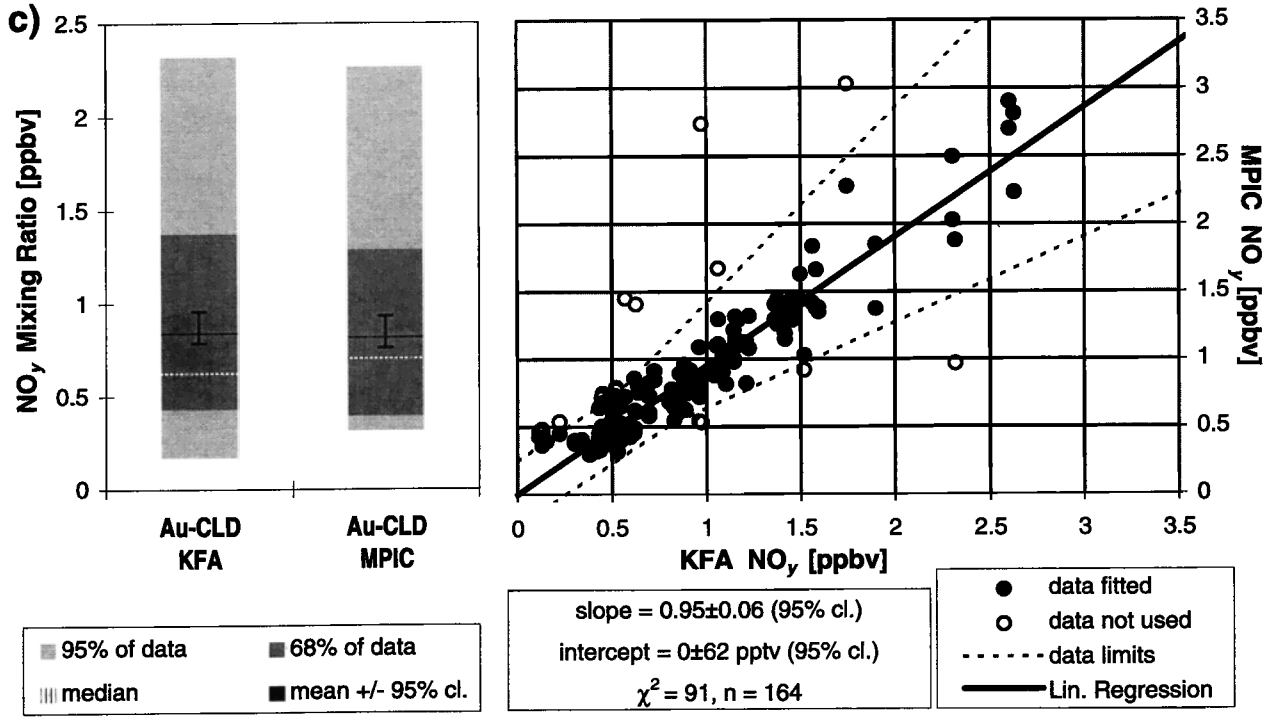

Figure 4. (continued)

data to be lower than KFA data (slope equal to 0.82±0.16). The NO_y in fresh pollution spikes from combustion sources is expected to consist solely of NO_x ($NO+NO_2$) which will not be as strongly affected by surface losses as HNO_3. Consistent with the overall data set and the proposed HNO_3 (or organic nitrogen oxide) losses, the data points at the low concentration end, for which HNO_3 represents the majority of NO_y (aged air), show a clear tendency toward higher MPIC values, while the few data points at the high concentration end, with a high NO_x, tend on average toward higher KFA values.

We therefore conclude that the MPIC instrument measured NO_y more reliably then the KFA instrument and therefore the 1-min KFA NO_y data set was corrected using the computed slope and intercept parameters, before averaging to the final 30-min data set in order to compensate for the HNO_3 inefficiency by comparison to the MPIC NO_y data. Consequently, the least squares fit between the final two 30-min data sets [*Stordal et al.*, 1995] yields a slope and intercept consistent with unity and zero (slope equal to 0.95±0.06, intercept equal to 0±62 pptv), respectively, as a result of this correction (Figure 4c).

3.5. Nitrogen Dioxide (NO_2)

3.5.1. Calibration. Gas phase titration of the NO calibration gas was used for calibration of the KFA PLC/CLD instrument (Volz-Thomas et al., submitted manuscript, 1997). For calibration of the MPIC TDLAS a NO_2 permeation source (VICI Metronics, NO_2-50F1-31583) that supplied 33.6 ng NO_2/min was dynamically diluted with N_2 gas to mixing ratios of typically 1.5 ppbv. A one-stage dilution system used flow controllers which were calibrated during the campaign. The setup was such that NO_2 did not contact any metal surface. The source has been monitored gravimetrically at the MPIC over the past three years and has been found to be stable within ±10% of the mean value with single weight loss measurements at intervals of 2-3 months. The accuracy of the NO_2-MIESR measurement is estimated to be 5% [*Mihelcic et al.*, 1985]. The MIESR and TDL NO_2 measurements were tied to each other by an intercalibration of a NO_2 tank (BOC 81599, nominal 10.0 ppmv) which was measured to be 8.60±0.43 ppmv and 8.88±0.22 ppmv (±1σ, N=29) by MIESR and TDL, respectively. An intercomparison between the NO_2 permeation source / NO_2 tank and the NO tank used with GPT to calibrated the KFA PLC/CLD instrument failed at the end of the Izaña campaign because the O_2 supply for the CL detectors ran out early. A later attempt to tie the NO_2 tank against the NO tank at the KFA institute failed because the NO_2 tank was accidentally depressurized.

3.5.2. Data sets and analysis. Because of degraded performance of the TDLAS instrument during this campaign [*Fischer et al.*, this issue], the scatter of the NO_2 2-min data was too high to allow a meaningful intercomparison. Thus only the 30-min averages were compared between PLC/CL and TDLAS measurements. For this analysis the acceptance criteria were applied as described in the NO section above. The data acceptance band parallel to the regression line was defined by ±100 pptv and ±20 pptv for MPIC and KFA, respectively, in order to include the data variability at the low concentration end. In addition, for the intercomparison with MIESR the PLC/CL and TDLAS data were averaged over the 23 individual 30-min MIESR sampling periods. The errors which are used in the fit are the observed variabilities, 20 pptv, 100 pptv, and 14 pptv for the PCL/CL, TDL, and MIESR data sets. The proportional calibration errors or the standard deviation of the averages were not used for reasons as discussed in the NO section. The estimated 14 pptv error for MIESR corresponds to the stated 5% accuracy of MIESR applied on the observed mean mixing ratio.

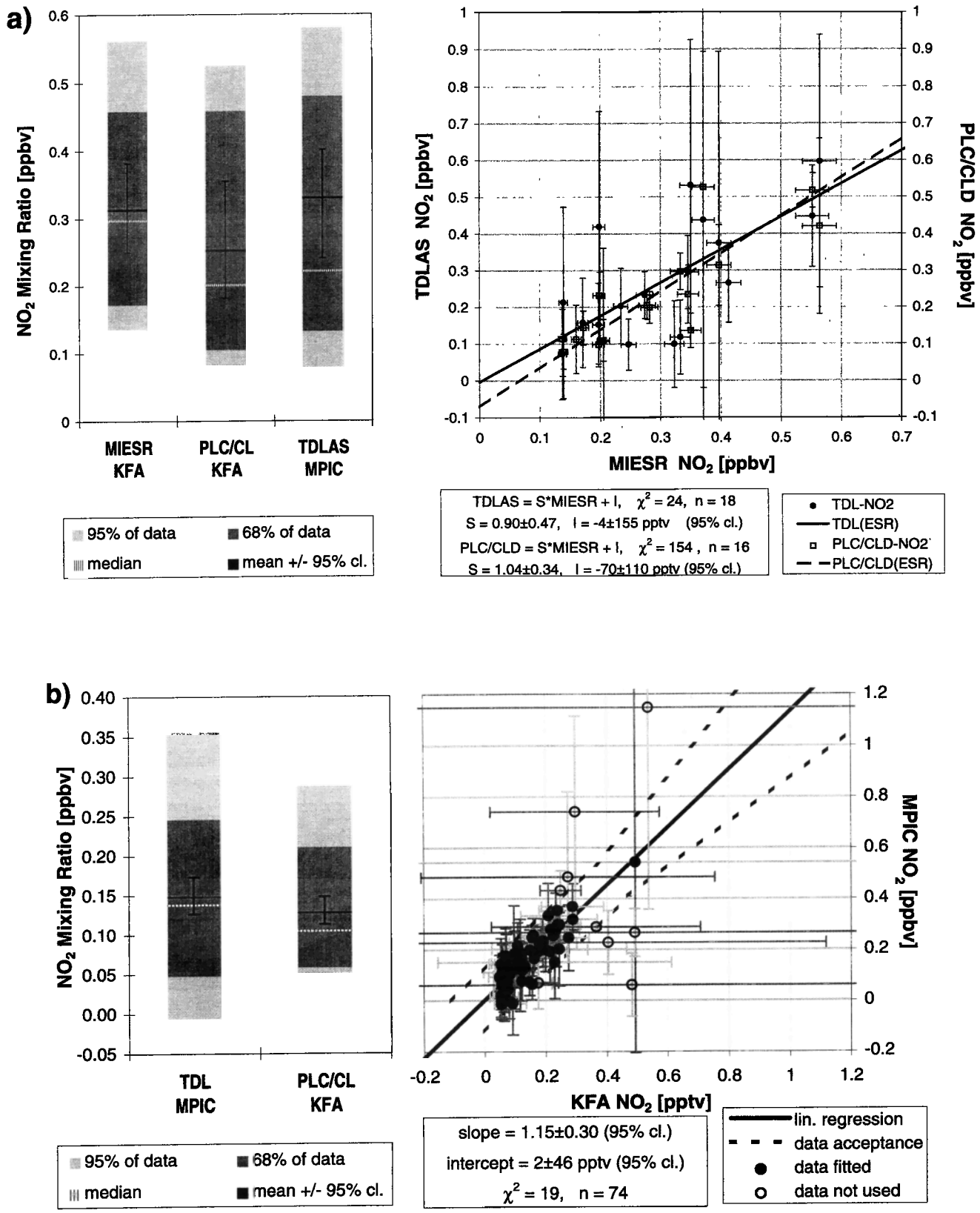

Figure 5. Intercomparison of nitrogen dioxide (NO_2) measurements. Left and right panels are as in Figure 2. Error bars are the standard deviation of the averaged 30-min samples. (a) NO_2 measurements obtained by KFA PLC/CLD and MPIC TDLAS instruments (30-min averages) versus KFA MIESR-Technique for 23 30-min MIESR samples (August 14-23). Linear least squares fits are indicated by a solid (TDLAS versus MIESR) and a dashed line (PLC/CLD versus MIESR). (b) A second data series: NO_2 measurements (30-min averages) obtained by MPIC TDLAS versus obtained by KFA PLC/CLD instruments (August 19/20).

3.5.3. Results and discussion. The TDL and PLC/CL measurements as compared to the MIESR NO_2 results are shown in Figure 5a. Both TDLAS and PLC/CL NO_2 techniques yield a most likelihood response within 10% of the MIESR technique, slopes equal to 0.90±0.47 and 1.04±0.34 (95% cl.), respectively. In the case of the PCL/CL versus MIESR analysis, the reported slope uncertainty of ±0.34 has been derived generating best fit conditions by increasing the individual errors by a factor of 4 since the low Q probability of the χ^2 parameter was not acceptable (see Table 2). This indicated much too low data variability estimates and subsequently, a not acceptable low slope uncertainty of ±0.10. Furthermore, no significant offset can be established. This is consistent with the confidence interval of the mean values overlapping each other, (Figure 5a, left panel, and Table 2). Figure 5b illustrates the intercomparison between NO_2 measurements by the MPIC TDLAS and the KFA PLC/CL method using a second, larger data set which is not covered by ESR samples (compare Table 2). The large variability, especially at the low concentration end, is caused by the large scatter of the TDLAS data. The acceptance criteria for data to be included in the regression analysis were chosen in order to include the data band at the low mixing ratio end, as discussed in the previous NO section. According to the fit results, the TDL data are 13%±30% (95% cl.) higher than those determined by the PLC/CLD, not including the 10% and 2% calibration uncertainties of the two data sets. Establishing best fit conditions by decreasing the individual data errors to 50% would lower the slope error from ±30% to ±15%.

Thus deviation from unity slopes in the NO_2 intercomparison is not more than expected. Furthermore, no significant offsets between the three methods can be detected (see Table 2).

On the CD-ROM [*Stordal et al.*, 1995], NO and NO_2 data were not published separately but rather a NO_x data set of 30-min averages was generated. Unfortunately, the combination of NO and NO_2 data including their sometimes different pollution spike patterns results in a less significant trend line than the NO_2 or NO data on there own. Thus a comparison of NO_x data would not add any additional information to this intercomparison.

3.6. Peroxy Radicals (RO_x)

3.6.1. Calibration. During operation, the calibrations of the chain length for the KFA and the two MPIC and IFE RO_x amplifiers were performed by adding quantitative amounts of HO_2 generated by photolysis of H_2O [*Schultz et al.*, 1995] and by thermal dissociation of PAN [*Hastie et al.*, 1991], respectively. The calibration of the NO_2 Luminox detectors were performed using a 8.6 ppmv NO_2 tank (BOC 81599, nominal 10.0 ppmv; see NO_2 section above) and two permeation sources for the KFA, MPIC, and IFE CAs, respectively (the NO_2 permeation sources were different to the one which was used for TDLAS). A NO_2 intercalibration was carried out using the NO_2 tank as reference. The mean ratios of the measured over the calculated NO_2 mixing ratios were 0.97 ± 0.06 (±7%, N=7), 1.18 ± 0.06 (±6%, N=7), and 1.13 ± 0.04 (±4%, N=2) for the KFA, MPIC, and IFE instruments (errors 1 standard deviation of the sample). This suggests some disagreement between the NO_2 tank and the permeation sources of 18% and 13%. Another test of the NO_2 calibration of the chemical amplifiers is the comparison of their NO_2 background signal with the ozone measurements made by the MPIC TE-49 or the KFA Dasibi. Because of NO added in large excess to the sampled air ambient, O_3 is quantitatively converted to NO_2 and registered as a NO_2 background signal together with ambient NO_2 (which is usually <1% of O_3 at Izaña). From this comparison one finds for the MPIC and IFE instruments that the CA NO_2 background signals are on average 15.3%±1.3% and 16.9%±0.4% higher, respectively, than the reported O_3 measurements which is consistent with the NO_2 calibration. For the KFA CA a meaningful comparison could not be extracted because a variation of the NO_2 background values of the order of ±30% was apparent compared to the O_3 measurements. The CAs are operated in a way that the CO reaction agent is switched on and off generating a modulated ΔNO_2 signal with the amplified RO_x signal as the modulation amplitude. Single point calibrations applying HO_2 or PAN in the concentration range between 30-100 pptv were performed which is in the measured daylight concentration range thus minimizing any possible nonlinearity of the amplifiers. Multipoint calibrations were not applied during the measurement periods since they are very time consuming and they were not considered as crucial at the time the OCTA campaign was carried out. The chain lengths were reported to be 36±5 (±14%) [*Schultz*, 1995], 37±20 (±52%), and 35±9 (±25%) (errors are 1 standard deviation of the calibration samples) for the KFA, MPIC, and IFE chemical amplifiers, respectively. The NO_2 calibration discrepancies will not effect the RO_x signals directly since these are calibrated directly with the PAN or HO_2 calibration sources assigning a calibrated RO_x amount to a certain ΔNO_2 amplitude. However, the known nonlinearity of the Luminox detectors can cause secondary errors if the NO_2 calibration is incorrect. These effects are estimated to result in about a 10% uncertainty in the radical signal, which is minor compared to the variation actually observed in the derived chainlengths of each instrument. The resulting overall estimate is that the deviation ranges between 17-53% which is the estimate of the overall performance variability of the chemical amplifiers (this includes any drifts of the NO_2 detectors). This is consistent with the estimate of about 50% derived from the daylight variability between the instruments over a period of 3 days shown in Figure 6. Very similar discrepancies were observed during the official Peroxy Radical Intercomparison Exercise (PRICE) made in 1994 at Schauinsland [*Volz-Thomas et al.*, 1996]. Whether one or the other instrument had a lower or higher variability should not be over interpreted since changes in some operational parameters might have played a role, for example, the IFE inlet line was cleaned or changed frequently which changed the inner surface conditions every time, while the cleaning of the MPIC inlet was reduced to a minimum and the KFA device was not cleaned at all during the measurement period in order to keep more constant operation conditions. On the other hand, Sahara dust events will likely have affected the MPIC inlet more than the frequently cleaned IFE inlet. The chain length of all the CAs was typically 50% shorter at the Izaña altitude than observed in prior laboratory tests, perhaps because of different flow conditions compared to those under normal pressure at sea level in the laboratories. Contamination of the inlet walls causing higher radical losses might have played a role, too. A multipoint RO_x intercalibration was tried but hampered by difficulties in adapting the HO_2 calibration source to the different CA inlets, especially under gusty wind conditions, as well as by improper design of the intercalibra-

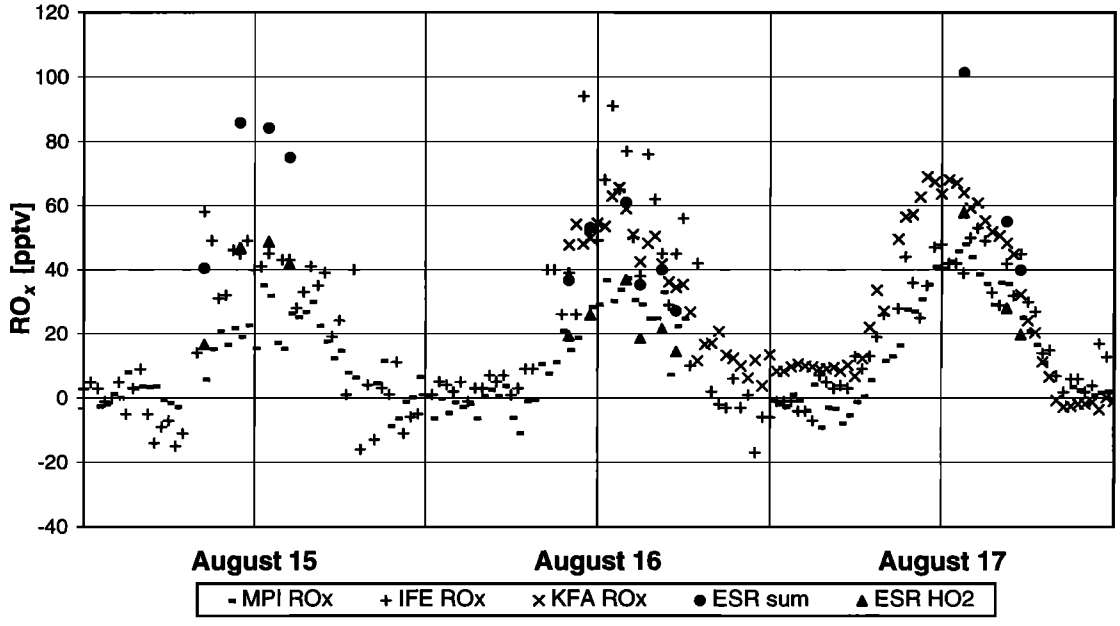

Figure 6. RO_x measurements time series for August 15-17. Displayed are 30-min averages. For the MIESR data points the total RO_x (ESR sum), and HO_x only (ESR HO_x) are displayed.

tion exercise. For several calibration points the HO_2 calibration gas was supplied well above 100 pptv. These measurements turned out to be meaningless since later investigations [*Schultz et al.*, 1995; *Heitlinger et al.*, 1995] showed that HO_2 mixing ratios should not exceed 100 pptv because of significant nonlinear losses due to the self reaction of HO_2 radicals above this level. As a result, no reliable calibrations could be derived from this experiment. Thus, the RO_x data could not be recalibrated to a primary RO_x calibration source.

3.6.2. Results and discussion. For all RO_x measurements 30-min averages were generated. A 3 day time series is displayed in Figure 6. The overall impression is that all instruments see a reasonable diurnal variation of the RO_x mixing ratios and that the daytime data agree within about 50%. This variability is consistent with the variability of the amplifier performance derived from the calibration data.

Some, but not all, of the MIESR total RO_x data samples are significantly higher than the CA data suggesting that during some metereological conditions the CA devices fail to detect some RO_x species seen by MIESR. The CA detectors measure only those RO_2 radicals which react with NO to produce a RO radical which subsequently reacts with oxygen to produce HO_2 ($RO + O_2 \rightarrow R'CHO + HO_2$). Larger RO_2 radicals which also react with NO to produce nitrates, $RONO_2$, are not expected to be observed by the CA detectors, while the MIESR technique should detect all peroxy radicals. The yield of the $RONO_2$ formation compared to the sum of $RONO_2$ and RO formation increases with the chain length of R and is estimated to be, for example, ~3% for propane, ~7% for pentane and butane, ~10% for isoprene and toluene, ~28% for heptane, and ~36% for octane [*Lightfoot et al.*, 1992]. Additionally, radical losses in the amplifier via $RO + NO \rightarrow RONO$ play a role for longer R chains [*Cantrell et al.*, 1993]. Experimental evidence for a decreased sensitivity of the CA toward organic radicals was obtained during measurements in the European Smog Chamber EUPHORE. The sensitivity for RO_x radical products from the ozonolysis of α-pinene was reported as <70% compared to the sensitivity for HO_2 [*Heitlinger et al.*, 1997].

There is evidence that during upslope wind conditions elevated levels of hydrocarbons and NO_x from anthropogenic sources as well as natural emissions from extensive eucalyptus and pine forests penetrate through the trade wind inversion at ~1500 m, well below the altitude of our observation site [*Schultz et al.*, this issue]. For example, up to 500 pptv pentane, 260 pptv butane, 160 pptv toluene, 800 pptv isoprene, and 100 pptv α-pinene were observed under upslope wind conditions [*Fischer et al.*, this issue, Table 2]. The bias due to different sensitivities of the CAs and the MIESR for the larger RO_2's would be severest for measurements taken under polluted conditions. Thus to minimize the potential effect on the statistical analysis, measurements with highest MIESR values, (3 on August 15, 1 on August 17, and 1 on August 21), were eliminated from the analysis. Additionally, very low MPIC values (~5 pptv) during the first four MIESR samples (~50 pptv) on August 14 were discarded.

The three CA data sets were statistically compared with the 23 MIESR samples, while the three CA instruments were compared to each other using a larger data set. A summary of the results is displayed in Figure 7 and listed in Table 2. The box and whisker bars in the lower right boxes of Figure 7 compare the data sets by their means and distribution. The upper left boxes display scatter plots of two pairs of data sets including a trend line resulting from the χ^2 fit (solid line) and a trend line forced through zero (dashed lines). The dashed lines contain the same information already display by the box and whisker bars since their slopes are the ratios of the means of the two data sets (S_0 in Figure 7).

Comparing the means of the data samples within their 95% confidence intervals, both the IFE and KFA CA means are consistent with the MIESR total RO_x means (S_0 is 1.01±0.20 and 0.98±0.24, respectively), while the MPIC CA mean is

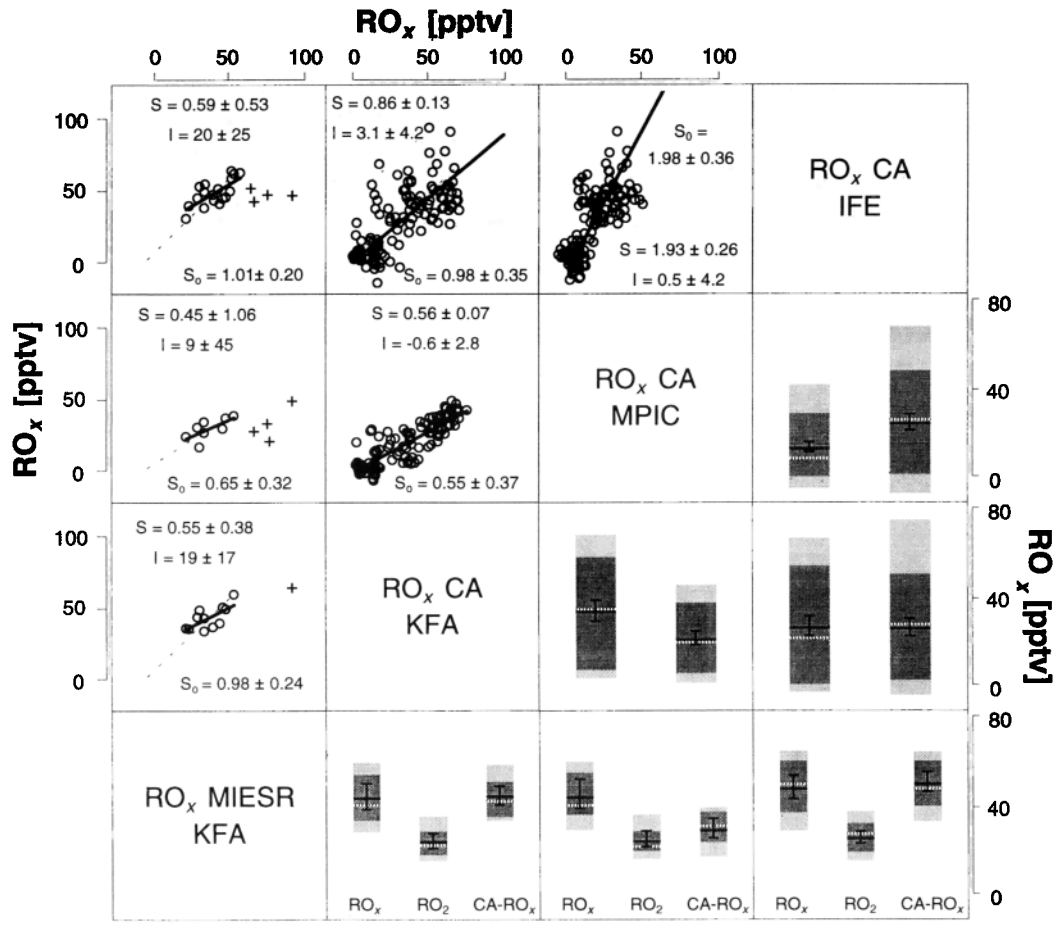

Figure 7. Means and correlation for the RO_x intercomparison. The diagonal boxes contain the axis titles for the off diagonal data boxes. The upper left data boxes show scatterplots and linear regressions between the RO_x data from the three chemical amplifiers (CA) and the MIESR technique (total RO_x used here). Slope S and intercept I refer to the linear χ^2 fit (solid line), and slope S_0 refers to the trend line forced through the origin (S_0 is equal to the ratio of the means of the two data sets). The title boxes below and to the right refer to the x axis and y axis, respectively. The lower right data boxes display statistics of the compared data in form of box and whisker bars as described in the Figure 2 caption. For the CA versus CA boxes the left and upper title boxes refer to the left and right bar, respectively. For the MIESR versus CA boxes the left two bars display the MIESR total RO_2 and HO_2, respectively, while the right bar displays the CA data referred to by the upper title box. The CA versus MIESR analysis is based on data pairs displayed a open circles (upper left boxes), while high ESR samples (plusses) are not included (see text).

significantly lower (S_0=0.65±0.32), falling between the MIESR HO_x and RO_x means. Consistent with this, the IFE and the KFA means agree with each other but not with the MPIC mean. There are two possible explanations: first, there might be a calibration bias with the MPIC CA instrument, or second, the MPIC CA is mainly sensitive to HO_2 and much less sensitive to higher peroxy radicals. The latter is unlikely since the design and operation parameters of the MPIC and IFA devices are very similar and the IFE mean agrees well with the ESR RO_x mean. Additionally, the two CAs are calibrated with the $CH_3C(O)O_2$ radical resulting from the PAN thermal decomposition. This excludes that the MPIC device is less sensitive to $R(C_1)O_2$ or $R(C_2)O_2$ radicals. On the other hand, we found no obvious calibration bias.

If the CA/MIESR data pairs with high MIESR values are included into the analysis, the ratios of the CA/MIESR means (S_0 values in Figure 7) will drop from 1.01, 0.98, and 0.65 to 0.88, 0.92, and 0.43 for the IFE, KFA, and MPIC CA, respectively. That is, for the entire MIESR data set, the IFE and KFA CAs come out ~10% low, which might be caused by different sensitivities to higher organic peroxy radicals as discussed above. These mean values of the entire data set still overlap with the MIESR RO_x means within their 95% confidence limits.

Additional linear fits of the CA data versus the MIESR data yield a most likelihood response of the order of 50% for the CA units compared to MIESR and one of them inconsistent with unity (95 cl.). (Figure 7 and Table 2). Decreasing the response uncertainty through decreasing the data variability estimates of the other two CA units as suggested by too high Q probabilities (Table 2) would make their response compared to MIESR inconsistent with unity, too. The low response of the CA units would suggest instrumental biases for the KFA and IFE CAs even though they agree with the

MIESR by their means (see ratio of responses as solid lines and ratio of means as dashed lines in Figure 7). However, constant daytime biases (offsets) between the instruments are not statistically significant, and a possible dependence of the chain length on the RO_x concentration is highly speculative at this point. In particular, for the CA/MIESR comparison, the dynamic range of the data is very small, and we have not obtained multipoint calibration data, which could verify such a trend. No dependency like this has been observed in the concentration range below 100 pptv by *Hastie et al.* [1991], by *Schultz* [1995], nor during PRICE [*Volz-Thomas et al.*, 1997], and not during recent laboratory calibration tests at IFE. Only for higher peroxy radical concentration their self-reaction might introduce some nonlinearity. In summary, the limited dynamic range of the data sets compared with the MIESR measurements, especially the data gap toward the origin does not allow any answer concerning a possible nonlinearity or daytime offset between the CA and the MIESR data. The assumed errors for the fits were the calibration accuracy of the instruments (see uncertainty of the chain lengths above and 5% for MIESR) applied on the mean values of the data. The calibration accuracy of the CAs is derived from the variability between calibrations which could result from real instrument instabilities. For reasons discussed in the NO section no standard deviations of the 30-min samples or proportional calibration errors were applied.

4. Summary and Comparison With Other Studies

During the European OCTA experiment, parallel measurements for NO, NO_2, NO_y, O_3, and RO_x were performed at Izaña (Tenerife) by several techniques, and intercalibrations were carried out. The measurement site is located on the Spanish island west of Africa is at 28°18'N, 16°30'W, and at 2370 m above sea level. For this data set, representing trace gas levels of the free troposphere and moderately polluted air from the boundary layer [*Fischer et al.*, this issue], intercomparisons of the data series and the different instruments and techniques were performed. The statistics of the intercomparison during this study are summarized in Table 2. The following summary refers to this table.

4.1. O_3

The two 1-min O_3 data series establish a significant difference in response between the two instruments of 7%±0.2% (95% cl.), so that an overall agreement between the two data sets can only be quoted within 7% at a 95% confidence level. The significant difference in response cannot be linked to the UV instruments but might have been caused by O_3 losses in one inlet line which was not protected by an aerosol filter. The significant 1 ppbv constant bias is within the instruments' specifications. The difference in the means reflects the linear bias (slope) between the two data sets. This well established in situ technique for O_3 is tied to known UV O_3 absorption cross sections and with normal maintenance no major error source will arise. Although, as observed during this campaign, inlet lines should be properly maintained and equipped with inline filters in order to minimize potential O_3 losses on the surface of the inlet, especially under conditions with high aerosol loads.

4.2. NO

The NO data obtained by two CL detectors are in very good agreement and thus are unaffected by the different materials used for the two inlet lines (stainless steel, glass, PFA). Over a mixing ratio range of 0-200 pptv the response of the two instruments agrees within 3%±10% at a 95% confidence level. A statistically significant ~15 pptv constant bias is probably due to an uncorrected offset of the MPIC instrument, as is the difference in the mean values. The significance of a 9% linear bias observed for the entire data set (0-6 ppbv) which included pollution spikes (at >200 pptv, <3% of the data) should not be over interpreted due to the poor statistics at the higher concentration end of the data set.

Earlier NO intercomparisons were reported from a ground-based campaign near Boulder, Colorado [*Fehsenfeld et al.*, 1987] and the airborne NASA GTE/CITE missions [*Hoell et al.*, 1985, 1987, 1990; *Gregory et al.*, 1990a]. In the work of *Fehsenfeld et al.* [1987], measurements of two CL instruments were compared. The authors report the measurements to be in good agreement (better than 10%) between 0.01-50 ppbv NO except for some periods with internal MoO_3 contamination from a Mo NO_y to NO converter. For the two lowest data bins containing 33 3-min averages, between approximately 13-70 pptv and 0.070-1.8 ppbv, the ratios can be estimated to be 1.10±0.45 (1σ) and 0.96±0.35 (1σ) ppbv [*Fehsenfeld et al.*, 1987, Figure 5], respectively. From the ground-based CITE 1 intercomparison [*Hoell et al.*, 1985] results are reported for two different mixing ratio ranges, 10-60 pptv (ambient air) and 20-170 pptv (ambient air plus added NO spikes), and from a third test under mainly constant mixing ratio with small spikes added . The average deviation of the regression slopes from unity for these three tests were 21%±23%, 16%±5%, and 10%±3% (1σ errors), respectively, between the three participating instruments. The authors conclude that the agreement among the instruments was in the 20%-30% range with a 30% accuracy at a 95% confidence limit. No significant biases were observed for ambient data (95% cl.), whereas during spiking tests (which would correspond to our pollution events), linear biases in the range of (15-30 ± 10)% were statistically significant (95% cl.). The airborne intercomparison CITE 1 and 2 with the same instruments are evaluated by *Gregory et al.* [1990]. For NO range of 0-70 pptv NO the slopes deviated from unity on average by 15%±26% (1σ) and 13%±15% (1σ) for CITE 1 and CITE 2, respectively.

Summarizing these former intercomparisons, they show slope deviations from unity between 10-30% with 2σ errors of 6-90% for NO ranges <170 and <70 pptv, and, for example, 4%±70% (2σ) for higher mixing ratios between 70-1800 pptv. In comparison, our result of 3%±10% (95% cl.) for NO <200 pptv represents an excellent agreement between two CL instruments which limits an observable systematic bias between the two CL detectors to this amount. It should be noted that this precision was achieved from statistics of a large data set over a several days period and over a concentration range of 0-200 pptv NO while the precision of individual 1-min NO measurements was approximately ±10 and ±100 pptv for the two detectors derived from nighttime variability.

4.3. NO_y

The significant differences between the original 1-min data sets are likely caused by losses of HNO_3 and/or organic nitro-

gen oxides in one of the inlet lines. Only indirect evidence could be found supporting this explanation since there were no measurements of HNO_3 and of organic nitrogen oxides other than PAN performed. However, the data show a confident correlation with a solely linear bias and we have no indication that similar losses the MPIC NO_y converter. The suggested HNO_3 losses of the KFA instrument were corrected in the final 30-min data set. Consequently the 30-min data set published on CD-ROM show an overall consistency.

A previous intercomparison of NO_y field measurements has been reported from the Boulder campaign where NO_y was measured over a range of 0.4-100 ppbv [*Fehsenfeld et al.*, 1987]. Two different NO_y to NO conversion techniques, based on Au and Mo catalysts, with subsequent CL detection of NO were employed. Besides reported problems with the Mo based system concerning memory effects and the above mentioned MoO_3 contamination problem, the data are reported to show good agreement above 1 ppbv NO_y for both converter types, while data for <1 ppbv gave no useful information due to calibration uncertainties. In this upper concentration regime a high portion of freshly emitted NO_x is to be expected. In contrast, NO_y compared during the MLOPEX 2 and NASA PEM-West A experiments [*Atlas et al.*, 1996] consisted of about 50% HNO_3 in the more aged and remote air masses around the Hawaiian Islands. NO_y means between 74 and 201 pptv have been reported using three different Au converters with subsequent NO detection by two CL detectors and a LIF technique. A difference between the mean values of about 20% (not significant within 2σ) and a disagreement of a factor of 3 were observed during two different measurement episodes, respectively. Similar to our data sets, inlet loss problems, especially regarding HNO_3, have likely played a major role [*Atlas et al.*, 1996; *Crosley*, 1994, 1996].

Currently, the NO_y conversion technique cannot be considered as reliable, especially in airborne applications where pressure and humidity changes in the inlet section can cause additional uncertainties. Measurements in high NO_x regimes are less problematic since the NO_2 to NO conversion is rather reliable and the subsequent NO detection is well established. In regimes with high HNO_3 content the inlet design seems to be the most critical factor and, to our knowledge, consistency between different instruments has not frequently been established.

4.4. NO_2

The intercomparison between the three applied measurement techniques agreed within 4%±34%, 10%±47%, and 13%±30% between PLC/CL-MIESR, TDL-MIESR, and TDL-PLC/CL, respectively, for a mixing ratio range of 55-670 pptv including MIESR data and 0-544 pptv between TDL-PLC/CL. TDL versus PLC/CL comprises a larger data set than that determined by the MIESR samples. Thus, as for NO, NO_2 sampling was not affected by the different materials used for the two inlet lines (stainless steel, glass, PFA) at this confidence level.

NO_x intercomparisons from the rural Boulder site, the CITE 2 mission [*Fehsenfeld et al.*, 1987; *Hoell et al.*, 1990; *Gregory et al.*, 1990b], and the PEM-West A / MLOPEX 2 comparison [*Atlas et al.*, 1996] have been reported. NO_2 to NO surface reduction using $FeSO_4$ as catalyst and a NO_2 to NO photolytical conversion technique were compared during the first intercomparison detecting NO by CL technique in both cases. The $FeSO_4$ method suffered from a constant bias of ~200 pptv which may be attributed to an interference to PAN and PAN-like constituents. During CITE 2 a $FeSO_4$/CL, a PLC/CL, a laser photolysis/LIF, and infrared absorption (tunable diode laser absorption spectroscopy, TDLAS) technique have been compared. For in-flight comparisons a level of agreement of the order of 30-40% among the instruments (maximum difference of the regressions slopes from unity) was reported for NO_2 measurements ranging between 0-200 pptv [*Gregory et al.*, 1990b]. From the data set it was suggested that the PAN conversion efficiency of the $FeSO_4$ technique could have been larger than 80% during some periods adding a significant offset to the NO_2 signal. Additionally, there was a positive offset of about 20-30 pptv apparent in the TDLAS data set compared to the other techniques. During the PEM-West A and MLOPEX 2 comparison, the NO_2 measurements of the airborne LIF instrument and the ground-based PLC/CL detector were reported comparable during the overflight period within the observed variation (data range 12-22 pptv). The difference of 2.6 pptv was within the standard deviation of the measurements. For measurements in the O_3 maximum a factor of 2 difference (equal to 13 pptv) was reported between the airborne and the ground-based measurement (data ranges 10-19 pptv and 21-30 pptv, respectively) which could not be explained. Thus our intercomparison gives a new evaluation between three different techniques with reasonable results over a range approximately 50-700 pptv. Below 50 pptv we cannot draw any save conclusion due to missing MIESR data and instrumental variability too high in the TDL data.

4.5. RO_x

The mean IFE-CA and KFA-CA RO_x values agree with the mean MIESR total RO_x to 1%±20% and 2%±24% (95% cl.). The MPIC CA mean comes out lower (35%±32%, 95% cl.) suggesting an unknown calibration bias or less likely, a reduced sensitivity to higher peroxy radicals of the MPIC CA device. The linear fit results of the CA versus the MIESR data might imply some constant offsets or nonlinearity between the instruments but they are too uncertain to draw any further conclusions, mainly due to low dynamic range of the data sets. However, the variability of the measurements on a 30-min time base is in the range of 50% (see Figure 6). A larger variability was observed during PRICE, 1994 at Schauinsland [*Volz-Thomas et al.*, 1997] under more polluted conditions.

5. Conclusions

The O_3 data sets exhibit a 7%±0.2% discrepancy, likely due to inlet losses in one inlet line which was not protected from dust contamination. O_3 is more sensitive to surface losses compared to for example, NO or NO_2, and if avoided, a higher accuracy for O_3 measurements can be obtained.

The excellent agreement of the NO measurements in the sub-200 pptv range within 3%±10% (95 cl.) improves earlier intercomparisons of CL instruments. For the photochemically sensitive sub-30 pptv range it would be beneficial to improve the current 30% confidence level [*Hoell et al.*, 1985, 1987, 1990] in this NO concentration range through additional intercomparisons between LIF and CL techniques. The NO_2 intercomparison gives some confidence in the 50-700 pptv

range for three different measurement techniques, MIESR, PLC/CL, and TDLAS of 4-13% (±30-47%, 95% cl.).

Earlier NO_x intercomparison experiments showed agreement in the range of 20-40% between different techniques [*Fehsenfeld et al.*, 1987; *Hoell et al.*,1990; *Gregory et al.*, 1990b; *Atlas et al.*, 1996]. Several of these techniques are capable of achieving detection limits <20 pptv, so that improvements of the NO_2 intercomparisons should be possible and would improve the reliability of NO_2 data for critical tests of photochemistry.

For NO_y, obvious inlet losses of one of the instruments and missing in situ HNO_3 conversion efficiency calibrations leave some open questions, although there is no evidence of inlet losses from laboratory tests using the specific design of the MPIC instrument. The NO_y intercomparison underlines the fact that the design of catalytic NO_y converters, especially of the inlet part, is critical, and that future automated calibrations with different NO_y components such as NO_2, HNO_3 and others, must be given a high priority. Similar conclusions were drawn from an earlier NO_y intercomparison [*Crosley*, 1994, 1996] obtained from measurements during MLOPEX 2 and NASA's PEM-West A. Field intercomparisons involving several converters with different designs should be organized to improve the understanding of these devices and improve their design as well as the operational parameters especially during airborne application.

Agreement of the RO_x measurements is within 50% during daylight conditions for 30-min averages, which is not accurate enough for critical test of the remote tropospheric photochemistry. Additional insight in the source of the uncertainties needs to be investigated by further intercomparison campaigns for these instruments. Nevertheless, this is the first field measurement intercomparison of RO_x measurement techniques and it gives a first critical insight in the performance of these instruments under field campaign conditions. The agreement is much better than observed during the PRICE campaign at Schauinsland which took place under more polluted conditions with a larger variety of RO_2 radicals [*Volz-Thomas et al.*, 1997].

Acknowledgments. The OCTA project was funded by the European Union under contract EV5V-CT91-0042. The development of the KFA chemical amplifier was supported by the German Research Ministry (BMBF) under grant 07EU723. During the data interpretation and analysis of this study, T. Zenker was also supported by NASA under cooperative agreement NCC-1-214 and contract NAGW-2929. Finally, we would like to thank two anonymous reviewers for helpful and thorough comments.

References

Atlas, E. L., and B. A. Ridley, The Mauna Loa Observatory Photochemistry Experiment: Introduction, *J. Geophys. Res., 101*, 14,531-14,541, 1996.

Atlas, E. L., et al., A comparison of aircraft and ground-based measurements at Mauna Loa Observatory, Hawaii, during GTE PEM-West and MLOPEX 2, *J. Geophys. Res., 101*, 14,599-14,612, 1996.

Bollinger, M. J., R. E. Sievers, D. W. Fahey, and F. C. Fehsenfeld, Conversion of nitrogen dioxide, nitric acid, and n-propyl nitrate to nitric oxide by gold-catalyzed reduction with carbon monoxide, *Anal. Chem., 55*, 1980-1986, 1983.

Cantrell, C. A., and D. H. Stedman, Possible technique for the measurement of atmospheric peroxy radicals, *Geophys. Res. Lett., 9*(8), 846-849, 1982.

Cantrell, C. A., R. E. Shetter, J. A. Lind, A. H. McDaniel, J. G. Calvert, D. D. Parrish, F. C. Fehsenfeld, M. P. Buhr, and M. Trainer, An improved chemical amplifier technique for peroxy radical measurements, *J. Geophys. Res., 98*, 2897-2909, 1993.

Crosley, D. R., Issues in the measurement of reactive nitrogen compounds in the atmosphere, *SRI Int. Rep. MP 94-035*, SRI Int., Menlo Park, Calif., 1994.

Crosley, D. R., NO_y Blue Ribbon panel, *J. Geophys. Res., 101*, 2049-2052, 1996.

DeMore, W. B., S. P. Sanders, D. M. Golden, R. F. Hampson, M. J. Kurylo, C. J. Howard, A. R. Ravishankara, C. E. Kolb, and M. J. Molina, Chemical Kinetics and Photochemical Data for the Use in Stratospheric modeling, *JPL Publ. 94-26*, 1994.

Drummond, J. W., D. H. Ehhalt, and A. Volz, An optimized chemiluminescence detector for tropospheric NO measurements, *J. Atmos. Chem., 2*, 287-306, 1985.

Fahey, D. W., C. S. Eubank, G. Hübler, and F. C. Fehsenfeld, Evaluation of a catalytic reduction technique for the measurement of total reactive odd-nitrogen NO_y in the atmosphere, *J. Atmos. Chem., 3*, 435-468, 1985.

Fehsenfeld, F. C., et al., A ground-based intercomparison of NO, NO_x, and NO_y measurement techniques, *J. Geophys. Res., 92*, 14,710-14,722, 1987.

Fischer, H., et al., Observations of high concentrations of total reactive nitrogen (NO_y) and nitric acid (HNO_3) in the lower arctic stratosphere during the Stratosphere-Troposphere Experiment by Aircraft Measurements (STREAM) II campaign in February 1995, *J. Geophys. Res., 102*, 23,559-23,571, 1997.

Fischer, H., et al., Trace gas measurements during the OCTA campaign 1993 at Izaña, *J. Geophys. Res.*, this issue.

Gregory, G. L., et al., An intercomparison of airborne nitrogen dioxide instruments, *J. Geophys. Res., 95*, 10,103-10,127, 1990a.

Gregory, G. L., J. M. Hoell Jr., A. L. Torres, M. A. Carroll, B. A. Ridley, M. O. Rodgers, J. Bradshaw, S. Sandholm, and D. D. Davis, An intercomparison of airborne nitric oxide measurements: A second opportunity, *J. Geophys. Res., 95*, 10,129-10,138, 1990b.

Harder, H., N. Houben, H.-W. Paetz, U. Platt, and A. Volz-Thomas, Messungen von Spurengasen und Photolyseraten während der FIELDVOC Kampagne in Pointe de Penmarc'h, Bretagne: Ein Beitrag zur Ozonbilanz, *Ber. des Forsch. Jülich, Jül-3144*, Forsch. Jülich, Jülich, Germany, 1995.

Hastie, D. R., M. Weißenmayer, J. P. Burrows, and G. W. Harris, Calibrated chemical amplifier for atmospheric RO_x measurements, *Anal. Chem., 63*, 2048-2057, 1991.

Heitlinger, M., H. Geiss, D. Mihelcic, P. Müsgen, H.-W. Pätz, M. Schultz, and A. Volz-Thomas, Messungen von Peroxiradikalen am Schauinsland über chemische Verstärkung, *Ber. Forsch. Jülich Jül-3047*, Forsch. Jülich, Jülich, Germany, 1995.

Heitlinger, M., A. Volz-Thomas, J. Wildt, K. Brockmann, S. Moenninghoff, and K. Wirtz, Formation of peroxy radicals during the ozonolysis of terpenes, in *7th European Symposium on Physico-Chemical Behaviour of Atmospheric Pollutants, The Oxidising Capacity of the Troposphere*, edited by B. Larsen et al., pp. 163-166, European Commission, Directorate-General XII, Brussels, Belgium, 1997.

Hoell, J. M., et al., An intercomparison of nitric oxide measurement techniques, *J. Geophys. Res., 90*, 12,843-12,851, 1985.

Hoell, J. M., G. L. Gregory, D. S. McDougal, A. L. Torres, D. D. Davis, J. Bradshaw, M. O. Rodgers, B. A. Ridley, and M. A. Carroll, Airborne intercomparison of nitric oxide measurement techniques, *J. Geophys. Res., 92*, 1995-2008, 1987.

Hoell, J. M., D. L. Albritten, G. L. Gregory, R. B. McNeal, S. M. Beck, R. J. Bendura, and J. W. Drewry, Operational overview of NASA GTE/CITE 2 airborne instrument intercomparisons: Nitrogen dioxid, nitric acid, and peroxyacetal nitrate, *J. Geophys. Res., 95*, 10,047-10,054, 1990.

Hoell, J. M., D. D. Davis, S. C. Liu, R. Newell, M. Shipam, H. Akimoto, R. J. McNeal, R. J. Bendura, and J. M. Drewry, The Pacific Exploratory Mission-West Phase A: September-October 1991, *J. Geophys. Res., 101*, 1641-1653, 1996.

Johnson, T. J., G. W. Harris, J. Bonifer, J. N. Crowley, T. Zenker, and H. Fischer, A TDLAS instrument for detection of stratospheric chlorine, *Geophys. Res. Lett., 23*, 3611-3614, 1996.

Kley, D., and M McFarland, Chemiluminescence detector for NO and NO_2, *Atmos. Technol., 12*, 63-69, 1980.

Lightfoot, P. D., R. A. Cox, J. N. Crowley, M. Destriau, G. D. Hayman, M. E. Jenkin, G. K. Moortgat, and F. Zabel, Organic peroxy radicals: Kinetics, spectroscopy and tropospheric chemistry, *Atmos. Environ., Part A, 26*(10), 1806-1963, 1992.

McKenna, D. S., A. Volz-Thomas, S. A. Penkett, G. Vaughan, H. Fischer, and F. Stordal, Oxidizing Capacity of the Tropospheric Atmosphere: Final report to the European Comission on contract EVSV-CT91-0042, European Commission, Brussels, Belgium, 1995.

Mihelcic, D., P. Müsgen, and D. H. Ehhalt, An improved method of measuring tropospheric NO_2 and RO_2 by matrix isolation and electron spin resonance, *J. Atmos. Chem., 3*, 341-361, 1985.

Mihelcic, D., A. Volz-Thomas, H. W. Pätz, D. Kley, and M. Mihelcic, Numerical analysis of ESR spectra from atmospheric samples, *J. Atmos. Chem., 11*, 271-297, 1990.

Press, W. H., S. A. Teukolsky, W. T. Vetterling, and B. P. Flannery, *Numerical Recipes in Fortran 77, The Art of Scientific Computing*, vol. 1, Cambridge Univ. Press, New York, 1996.

Ridley, B. A., and E. Robinson, The Mauna Loa Photochemistry Experiment, *J. Geophys. Res., 97*, 10,285-10,290, 1992.

Roths, J., T. Zenker, U. Parchatka, F. G. Wienhold, and G. W. Harris, Four-laser airborne infrared spectrometer for atmospheric trace-gas measurements, *Appl. Opt., 35*, 7075-7084, 1996.

Schultz, M., Die Bedeutung von Stickoxiden für die Ozonbilanz in Reinluftgebieten, Ph.D. thesis, Bergische Univ.-Gesamthochschule Wuppertal, Wuppertal, Germany, 1995.

Schultz, M., M. Heitlinger, D. Mihelcic, and A. Volz-Thomas, A calibration source for peroxy radicals with built-in actinometry using H_2O and O_2 photolysis at 185 nm, *J. Geophys. Res., 100*, 18,811-18,819, 1995.

Schultz, M., R. Schmitt, K. Thomas, and A. Volz-Thomas, Photochemical box-modeling of long-range transport from North America to Tenerife during NARE 1993, *J. Geophys. Res.*, this issue.

Stordal, F., C. W. Tellefsen, and S. Skaug, Observational data from the project Oxidizing Capacity of the Tropospheric Atmosphere (OCTA) 1992/94, CD-ROM Database, *Norw. Inst. for Air Res.*, Lillestrom, Norway, 1995.

Volz-Thomas, A., et al., Peroxy Radical InterComparison Exercise (PRICE), in *Proceedings of Eurotrac '96*, edited by P. M. Borrell et al., pp. 621-625, Comput. Mech., Billerica, Mass., 1996.

Volz-Thomas, A., et al., Photo-oxidants and precursors at Schauinsland, Black Forest: Chemistry and transport, in *Tropospheric Ozone Research*, edited by X. Hov, pp. 322-332, Springer, Berlin, Germany, 1997.

Zenker, T., A. M. Thompson, D. P. McNamara, T. L. Kucsera, G. W. Harris, F. G. Wienhold, P. LeCanut, M. O. Andreae, and R. Koppmann, Regional trace gas distribution and airmass characteristics in the haze layer over southern Africa during the biomass burning season (September/October 1992): Observations and modeling from the STARE/SAFARI-92/DC-3, In *Biomass Burning and Global Change*, edited by J. Levine, pp. 296-308, MIT Press, Cambridge, Mass., 1996.

Zitzelsberger, R., Photochemische Ozonproduktion in ländlichen Gebieten Süd-West-Europas, Ph.D. thesis, Ruprechts-Karls-Univ. Heidelberg, Heidelberg, Germany, 1997.

T. Zenker, Department of Physics, Hampton University, Hampton, VA 23668. (e-mail: zenker@lily.larc.nasa.gov)

H. Fischer, C. Nikitas, and U. Parchatka, Air Chemistry Department, Max-Planck-Institut für Chemie, Postfach 3060, D-55020 Mainz, Germany. (e-mail: hofi@mpch-mainz.mpg.de; up@mpch-mainz.mpg.de)

G. W. Harris, Centre for Atmospheric Chemistry, York University, North York, Ontario M3J 1P3, Canada. (e-mail: gharris@yorku.ca)

D. Mihelcic, P. Müsgen, H. W. Pätz, and A. Volz-Thomas, ICG2, Forschungszentrum Jülich, Postfach 1913, D-52425 Jülich, Germany. (e-mail: d.mihelcic@fz-juelich.de; p.muesgen@fz-juelich.de; h.paetz@fz-juelich.de; a.volz-thomas@fz-juelich.de)

M. Schultz, Center for Earth and Planetary Sciences, Harvard University, Cambridge, MA 02138. (e-mail: mgs@io.harvard.edu)

R. Schmitt, Meteorologie Consult GmbH, Auf der Platt 47, D-61479 Glashütten, Germany. (e-mail: 100060.2416@compuserve.com)

T. Behmann, M Weißenmayer, and J. P. Burrows, Institut für Umweltphysik, Universität Bremen, Postfach 330440, D-28334 Bremen, Germany. (e-mail: behmann@iup.physik.uni-bremen.de; burrows@iup.physik.uni-bremen.de)

(Received, March 10, 1997; revised, December 9, 1997;
accepted December 9,1997.)